AD-A082 641 NORTHROP CORP DES PLAINES IL DEFENSE SYSTEMS DIV F/G 9/5
PARAMETRIC OSCILLATIONS IN HIGH POWER MICROWAVE AMPLIFIERS.(U)
1979 G DOHLER F49620-77-C-0096
UNCLASSIFIED AFOSR-TR-80-0228 NL

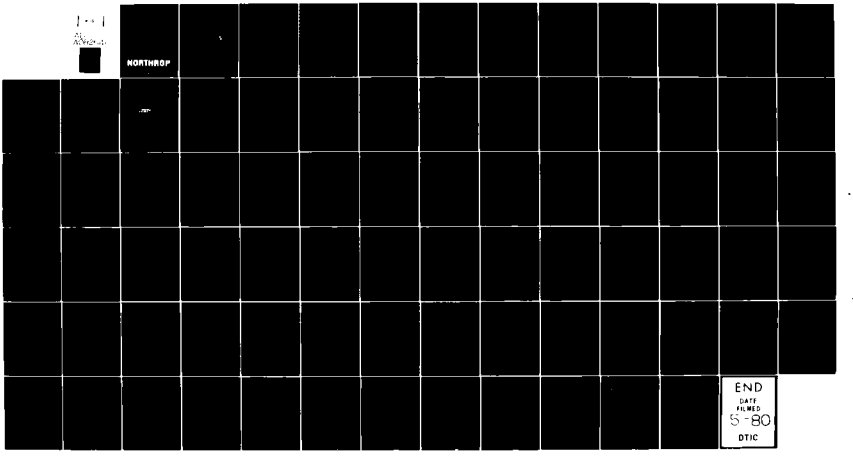

END
DATE FILMED
5-80
DTIC

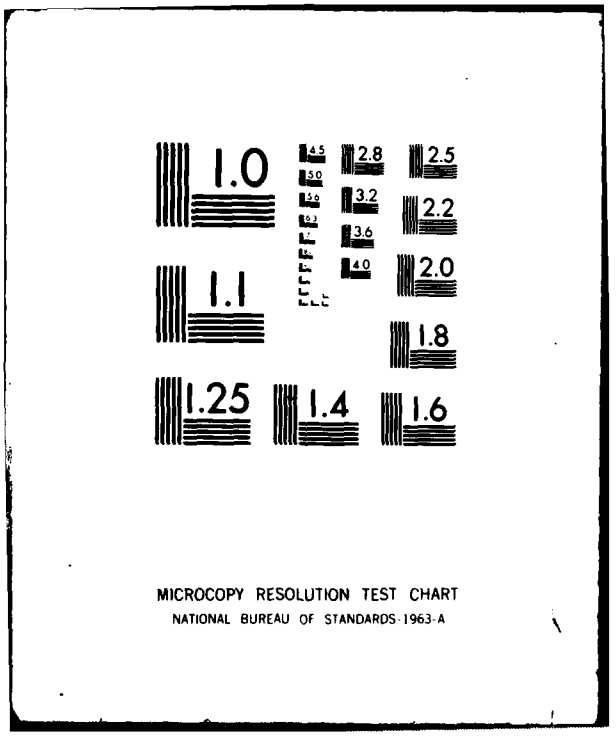
1.0
1.1
1.25
1.4
1.6
1.8
2.0
2.2
2.5
2.8
3.2
3.6
4.0
4.5
5.0
5.6
6.3
MICROCOPY RESOLUTION TEST CHART
NATIONAL BUREAU OF STANDARDS-1963-A

LEVEL II

PARAMETRIC OSCILLATIONS IN HIGH POWER MICROWAVE AMPLIFIERS

NORTHROP

Northrop Corporation

Defense Systems Division

(3)

PARAMETRIC OSCILLATIONS

IN HIGH POWER MICROWAVE AMPLIFIERS

Contract No. F49620-77-C-0096

Final Report

July 1977 to June 1979

Prepared by: Dr. Gunter Dohler

Northrop Corporation
Defense Systems Division
Electron Tube Section
175 W. Oakton Street
Des Plaines, IL 60018

TABLE OF CONTENTS

TABLE OF CONTENTS (CON'T)

LIST OF FIGURES

1.0 INTRODUCTION

High power microwave amplifier tubes, including injected beam crossed field amplifiers (IBCFA's) and broad band traveling wave tubes (TWT's) may exhibit several types of spurious signals in their output power spectrum. This paper describes one class of spurious signals, called parametric oscillations, for which a mathematical model is proposed.

By charting the frequency f_{sp} of the parametric signals as a function of drive frequency f_d, an empirical relationship is obtained:

$$f_{sp} = mf_o - nf_d \tag{1}$$

where n and m are positive or negative integers. f_o is a fixed frequency which is correlated empirically to a limit frequency in the stopband of the slow-wave structure. Figures 1 and 2 show typical measured data obtained from an S-band IBCFA and a Ku-band TWT.

Relation (1) seems to indicate that the origin of these oscillations is due to intermodulation products between two signals in the amplifier. Assuming that the spurious signals are intermodulation products between the signal frequency and an oscillation inherent in the tube at the frequency f_o, then one would expect to find a coherent oscillation in the absence of the injected signal (drive). Such is not the case. In fact, high drive power levels are required for these oscillations to occur. Figure 3 illustrates this behavior. Here, the amplifier is driven at a frequency of 3.9GHz, and the lower edge of the circuit stopband is known to occur at 7.8GHz. The upper right picture of the spectrum analyzer display (Figure 3) shows a normal clean

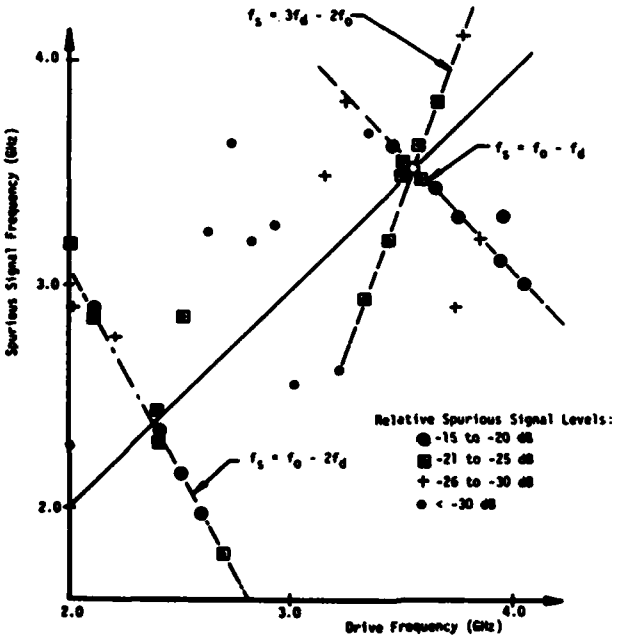

Fig. 1. Spurious signals in IBCFA.

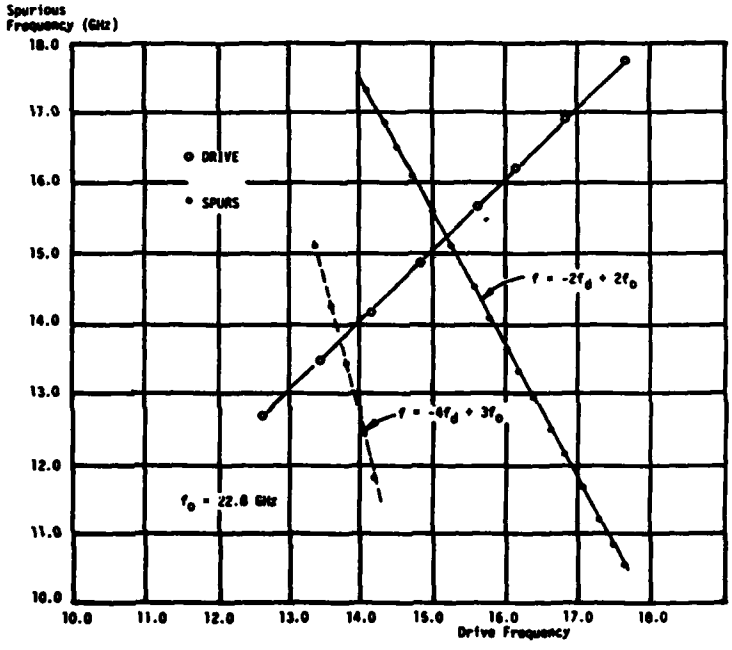

Fig. 2. Spurious oscillations in *Ku*-band TWT.

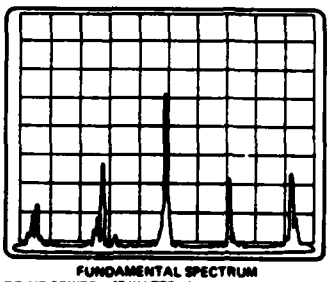

FUNDAMENTAL SPECTRUM
DRIVE POWER: 46 WATTS; OUTPUT POWER: 1 kW

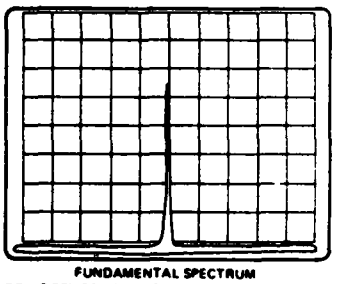

FUNDAMENTAL SPECTRUM
DRIVE POWER: 32 WATTS; OUTPUT POWER 1 6 kW

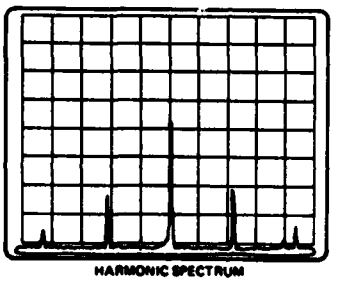

HARMONIC SPECTRUM

OUTPUT POWER SPECTRUM

DRIVE FREQUENCY:	3 9 GHz
HARMONIC:	7.8 GHz
50 MHz/DIVISION	(Horizontal)
10 dB/DIVISION	(Vertical)

Fig. 3. Output power spectrum.

output power spectrum from the amplifier driven close to (or just into) saturation (drive power level 32W). The output power is measured to be 1.6kW.

The photograph in the upper left hand corner of Figure 3 shows the spectrum containing the spurious signals when the amplifier is driven into hard saturation (drive power level = 45W). The photograph in the lower left corner of Figure 3 shows the output spectrum appearing under these same conditions at the harmonic frequency of 7.8GHz. The output power dropped from 1.6 to 1kW at the signal frequency, resulting in a "power-suckout" frequently observed in TWT's and CFA's.

Since the spurious signals are only observed under full beam power conditions and with the presence of a drive signal, preferably at high power, it is believed that the amplifier is pumped by a signal related to the drive signal, similar to a parametric amplifier. Hence, we have coined the term "parametric oscillations" to describe these spurious signals.

A model which describes parametric oscillations must be based on the existence of a) a full power electron beam, b) a strong RF drive signal, and c) a periodic structure.

A model, fulfilling these three requirements, was proposed to the Air Force Office of Scientific Research for further evaluation, and sponsored by the agency from July 1977 to June 1979. The first phase of the study program applied the model to injected beam crossed field amplifiers. The model predicted the simultaneous existance of very low frequency oscillations, which have been detected experimentally. These results, which have been

discussed in detail in an interim report submitted to AFOSR[1], in publication[2] and at the IEDM meeting in Washington, 1978[3], will be summarized in this report.

The second phase of the program applied the model to helix type traveling wave tubes. The results obtained will also be presented in this final report.

---

1) G. Dohler, Parametric Oscillations in High Power Microwave Amplifiers, Contract No. F49620-77-C-0096 (1979).

2) O. Doehler, G. Dohler, IEEE Transactions on Electron Devices, ED 26(10), 1602 (1979).

3) O. Doehler, G. Dohler, International Electron Devices Meeting, Washington, D.C. (Dec. 1978).

2.0 THE BASIC MODEL

The delayed electromagnetic wave in a slow wave microwave amplifier propagates in a space with an effective dielectric constant ε which is determined by the geometric properties of the periodic slow wave structure and the space "above" the line which contains the electron beam. In operation, the electron beam is modulated in time and space due to the electron bunches passing above the line, so that interactions with the RF wave can occur. The volume occupied by the electron bunches will therefore present to the RF wave a time and space dependent dielectric constant. It is therefore expected that the effective "hot" dielectric constant ε of the slow wave structure will also depend on the time and space dependent space charge in the beam, and is given by:

$$\varepsilon = \bar{\varepsilon}\,(1 + \delta\Delta\rho/\rho_0) \tag{2}$$

$\Delta\rho = \Delta\rho(r,t)$ = time- and space dependent space charge

ρ_0 = dc space charge

δ = geometric factor

If one assumes now that the depth of modulation $\Delta\rho/\rho_0$ is constant*, and that the beam is propagating in z-direction, then $\Delta\rho$ can be developed in a Fourier series:

$$\varepsilon = \bar{\varepsilon}\,[\,1 + \Sigma\,\delta_m \exp jm\omega_d(t - z/v_e)] \tag{3}$$

ω_d = drive frequency (of delayed wave)

v_e = average electron velocity in z-direction

* In operation, the depth of modulation increases with z until saturation occurs. The assumption, therefore, holds over most of the line in overdrive condition, and was used here only to simplify the discussion.

The effective dielectric constant is, therefore, modulated with all the harmonics of the drive frequency. If one simplifies further by considering only the main Fourier component:

$$\varepsilon = \bar{\varepsilon}\,[\,1 + \delta_m \cos \omega_p(t - z/v_e)] \tag{4}$$

$$\omega_p = m\omega_d$$

then it is seen that the effective dielectric constant is modulated with a pump frequency $f_p = mf_d$. Even though the coefficient δ_m in Relation (4) may be small compared to 1, the existence of waves at frequencies ω_p in or close to the stopbands, induces resonances in each periodic section of the periodic wave structure, which are more pronounced with wide stopbands, and thus may introduce further modulation of the beam at this frequency.

As required, this model is based on a) the presence of the electron beam, perferably at full power, b) the presence of a drive signal, preferably in overdrive condition and c) the existence of a periodic structure with a stopband.

3.0 THE CFA DELAY LINE

3.1 The Physical Model

Figure 4 shows schematically the interaction space of a crossed field amplifier (CFA). The slow wave structure is a meander line, the individual fingers of which are supported by ceramic bars. The individual fingers are connected to adjacent ones at opposite ends by an "empty waveguide" section (not supported by ceramic bars). The electron beam above the line is injected from a cathode (not shown), and remains above the line by means of a crossed dc electromagnetic field E_o (y-direction) and B_o (x-direction) which forces the beam to move in z-direction with a velocity $v_e = E_o/B_o$. Each individual finger of the slow wave structure is therefore perpendicular to the velocity of the electrons. As a result, each individual finger n will be subjected to a purely time dependent dielectric constant, shifted from the adjacent ones by a phase constant phase $\pm\omega_p P/v_e$, where P is the true pitch (in z-direction) of the line:

$$\epsilon_{(n)} = \bar{\epsilon}\,[\,1 + \delta_m \cos \omega_p(t - nP/v_e)] \qquad (5)$$

If one now "stretches" the meander line, one obtains a waveguide (microstrip line) which is periodically loaded by a dielectric of length ℓ_1, as schematically shown in Figure 5. By doing this, one effectively neglects the coupling between the bars, but the frequency position of the band gap is preserved. Thus, the model of the CFA, as shown in Figure 5, is a periodically loaded waveguide the dielectric sections of which have a time dependent effective dielectric constant as given by relation (5).

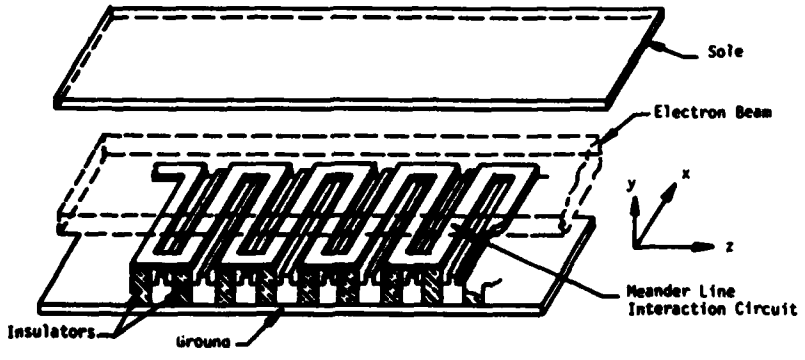

Fig. 4. Schematic of the interaction space in CFA's.

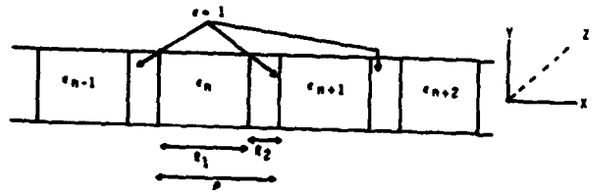

Fig. 5. IBCFA model analyzed.

3.2 The Mathematical Model

To analyze the line as schematically shown in Figure 5, one must first solve the wave propagation in a single section, the dielectric of which is periodically modulated with a pump frequency f_p. Once the solution has been found for a single section, boundary conditions at the interfaces of the dielectric with the vacuum section must be introduced. As a result, a transfer matrix connecting the fields at the entrance of a single dielectric section n to the fields at the entrance of the next dielectric section n+1 can be found. By multiplying this matrix by itself N times, where N is equal to the number of individual fingers (approx. 96), the entire transfer matrix of the line can be found.

3.2.1 Mathematical Solution in a Dielectric Section

The equations governing the propagation of an RF wave in a waveguide are given for a TEM mode by Maxwell's equations:

$$\partial E/\partial x = -\mu \partial H/\partial t \qquad \partial H/\partial x = {}^{+}\partial \epsilon E/\partial t \tag{6}$$

which can be combined by introducing $D = \epsilon E$, since ϵ is only time dependent in a single dielectric section

$$\partial^2 D/\partial x^2 = \epsilon\mu \partial^2 D/\partial t^2$$

This equation is solved by the method of variable separation [$D = D_1(x)D_2(t)$] by introducing a propagation constant β

$$D_1''(x)/D_1(x) = -\beta^2 = \epsilon\mu D_2''(t)/D_2(t) \tag{7}$$

which leads to the solution

$$D_1(x) = a \exp j\beta x + b \exp - j\beta x$$

together with Hill's equation

$$D_2''(t) + (\beta^2/\varepsilon\mu)D_2(t) = 0$$

Using the dc term of the dielectric constant as well as the maximum of the Fourier component ($\delta \ll 1$)

$$\frac{1}{\varepsilon} \simeq \frac{1}{\varepsilon}[1 - \delta \cos(\omega_p t - \phi)]$$

one obtains Mathieu's equation by properly time shifting

$$D_2''(t) + \beta^2 v^2 (1 - \delta \cos \omega_p t) D_2(t) = 0$$

From Floquet's theorem it follows that one solution is given by

$$F_\nu(t) = e^{j\,t_P(t)} \qquad P(t) = \Sigma C_n e^{jn\omega_p t}$$

where the characteristic exponent ν has to be determined. In general, but not necessarily, $F_\nu(-t)$ is also a solution of Mathieu's equation which is linearly independent of $F_\nu(t)$. Thus in general

$$Ae^{j\nu t}\Sigma C_n e^{jn\omega_p t} + Be^{-j\nu t}\Sigma C_n e^{-jn\omega_p t} \tag{8}$$

is a complete solution for $D_2(t)$. Since $|\delta|$ is small as compared to one, ν is generally real except for $2\beta v \simeq n\omega_p$, which will be excluded, since no wave growing exponentially in time is observed.

From the solution obtained it follows that, for a single propagation constant $\beta(\approx \omega/v)$ an infinite number of waves with frequencies $\omega_n = \omega + n\omega_p$ will propagate. The case $\omega = n\omega_p/2$ must be treated separately.

3.2.2 Physical Interpretation and Simplification

3.2.2.1 Injection of a Single Wave

Let us assume now that a single wave of frequency f is injected into the first section of the line. Due to the pump frequency, an infinite number of waves with frequencies $f_n = f \pm nf_p$ and with the same propagation constant β will propagate in the dielectric section, and exit this section on both sides. Consequently, the second dielectric section will "receive" and reflect an infinite number of waves with frequencies f_n. These waves will transmit through the second dielectric section with both the initial propagation constant β and their eigen-value $\beta_n = 2\pi f_n/v$.

In principle, therefore, one must track an infinite number of waves injected from both sides of each dielectric section. However, since the amplitude of the waves of frequency f_n generated in the first section, reflected and transmitted by this section decreases rapidly with increasing value of n, it is therefore practical to consider only values $n = 0$ and $n = \pm 1$.

3.2.2.2 Injection of Two Waves: Active and Passive Coupling

Let us now consider the case of two waves with frequencies f_1 and f_2 injected into the first section. In this first section then, waves with frequencies $f_1^{\pm} = f_1 \pm f_p$ and $f_2^{\pm} = f_2 \pm f_p$ will be generated. If the two primary frequencies f_1 and f_2 are such that $(f_1 < f_2)$:

$$f_1 + f_2 = f_p \tag{9}$$

then these two waves will be actively coupled*. If, however

$$f_2 - f_1 = f_p \tag{10}$$

then, these waves are passively coupled. The differentiation between these coupling modes is made because two waves

$$\phi_1(x)e^{j\omega_1 t} \quad \text{and} \quad \phi_2(x)e^{j\omega_2 t}$$

which are passively coupled will be coupled directly

$$e^{j(\omega_1 + \omega_p)t} = e^{j\omega_2 t}$$

$$e^{j(\omega_2 - \omega_p)t} = e^{j\omega_1 t}$$

while those actively coupled will be coupled indirectly through their conjugate complex values

$$e^{j(\omega_1 - \omega_p)t} = e^{-j\omega_2 t} = (e^{j\omega_2 t})^*$$

$$e^{j(\omega_2 - \omega_p)t} = e^{-j\omega_1 t} = (e^{j\omega_1 t})^*$$

3.2.2.3 Presence of Three Waves and Boundary Conditions

The case analyzed assumes three primary waves f_1, f_2, f_3 to propagate in the CFA delay line, two of which are actively coupled and two of which are passively coupled

$$f_1 + f_2 = f_p \qquad f_3 - f_1 = f_p. \tag{11}$$

The simplification $n = 0, \pm 1$ leads then to the presence of six waves within

* The terminology of active and passive coupling has been taken from Louisell's work[4]. Although the present theory, described in detail in 1), 2) and 3) is more general since β is not necessarily equal to $\sqrt{\epsilon}\,\omega/c$, this terminology has been kept here.

4) W.H. Louisell, Coupled Mode and Parametric Electronics, New York; Wiley (1960).

the CFA lines, three waves propagating in each direction (forward and backward). Each of these waves is actively or passively coupled to other waves, and is reflected or transmitted at each of the boundaries between the dielectric and the vacuum of each section. The mathematical computation, therefore, requires the tracking of six waves, each wave being characterized by two coefficients (amplitude and phase). This requires 12 x 12 transmission matrices. The computer program used requires as input conditions the geometry of the delay line and the knowledge of three incoming waves (amplitudes $A_1^+(f_1)$, $A_2^+(f_2)$, $A_3^+(f_3)$). Furthermore, their relative phases ϕ_1, ϕ_2 and ϕ_3 must be given. It is assumed that the line is perfectly matched at the input and output (no reflections from the input and output connectors). Knowing the pumping phase ϕ_p required between two adjacent bars

$$\phi_p = \omega_p P/v_e \tag{12}$$

the amplitudes $A_1^-(f_1)$, $A_2^-(f_2)$, and $A_3^-(f_3)$ reflected from the line at the input as well as the amplitudes $B_i^+(f_i)$ transmitted through N sections can be calculated (see Figure 6).

3.3 Computer Results

The computer results obtained are summarized herein by discussing the most pertinent results.

3.3.1 Results Obtained with CFA Line

The pump frequency f_p was continuously varied between 10 and 15GHz, since the bandgap of the unfolded meander line was calculated to be between 12.8 and 13.7GHz. The frequency f_1 was varied between the frequencies 200MHz and

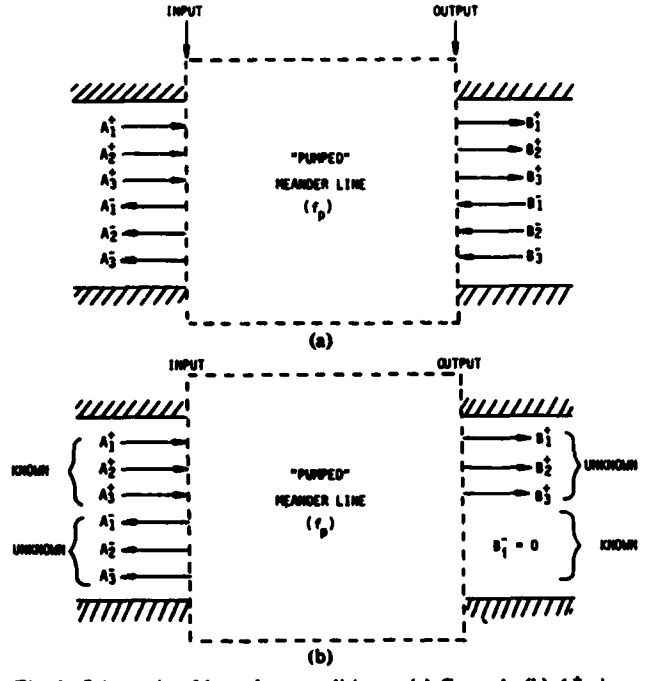

Fig. 6. Schematic of boundary conditions. (a) General. (b) A_j^+ given. $B_j^- = 0$ set.

f_p - 200MHz. The input conditions

$$A_i^+ = 1$$

were used, and the pump phase ϕ_p continuously varied. The total output power $P_i = (A_i^-)^2 + (B_i^+)^2$ for each wave of frequency f_i was monitored. It became rapidly clear that $P_i > 10$ could only be obtained when both f_1 was close to f_p, and f_p, the pump frequency in the bandgap, leading to a large power gain at f_2. Varying the pump phase ϕ_p between bars lead to an increase of P_2 above 100, and for $\phi_p = \pi$, the result of Figure 7 was obtained. The following two conclusions can be drawn:

1) Power gain is substantial at low values of $f_2 (f_1 \approx f_p)$.
2) As the pump frequency f_p is increased, the value f_2 for which P_2 becomes maximum also increases

$$f_{2max} = f_p - f_{1max} = f_p - f_o \qquad (13)$$

where f_o is a fixed frequency which can be determined from Figure 7 to be

$$f_o = 12.8\text{GHz}$$

which is just the lower edge of the bandgap.

The input conditions were changed by increasing the value of A_2^+ from 1 to 500, leaving A_1^+ and A_3^+ equal to 1. No appreciable power gain was obtained. However, increasing A_1^+ to 500, leaving $A_2^+ = A_3^+ = 1$ led to a power gain for f_2 of more than 80dB, see Figure 8. Here again, the frequency $f_o = 12.8$GHz is clearly detected. Note also that about 20dB gain is obtained at f_3 (high frequency).

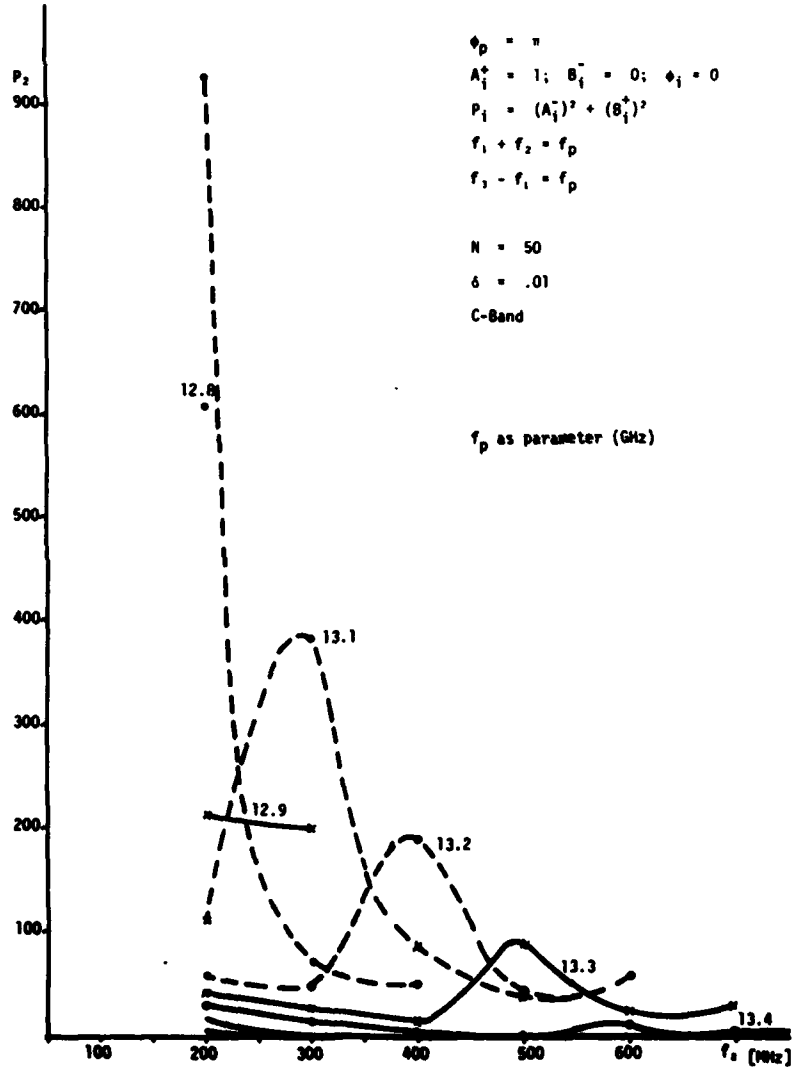

Fig. 7. Total output power P_2 versus frequency $f_2 = f_p - f_1$ (f_p close to or in bandgap).

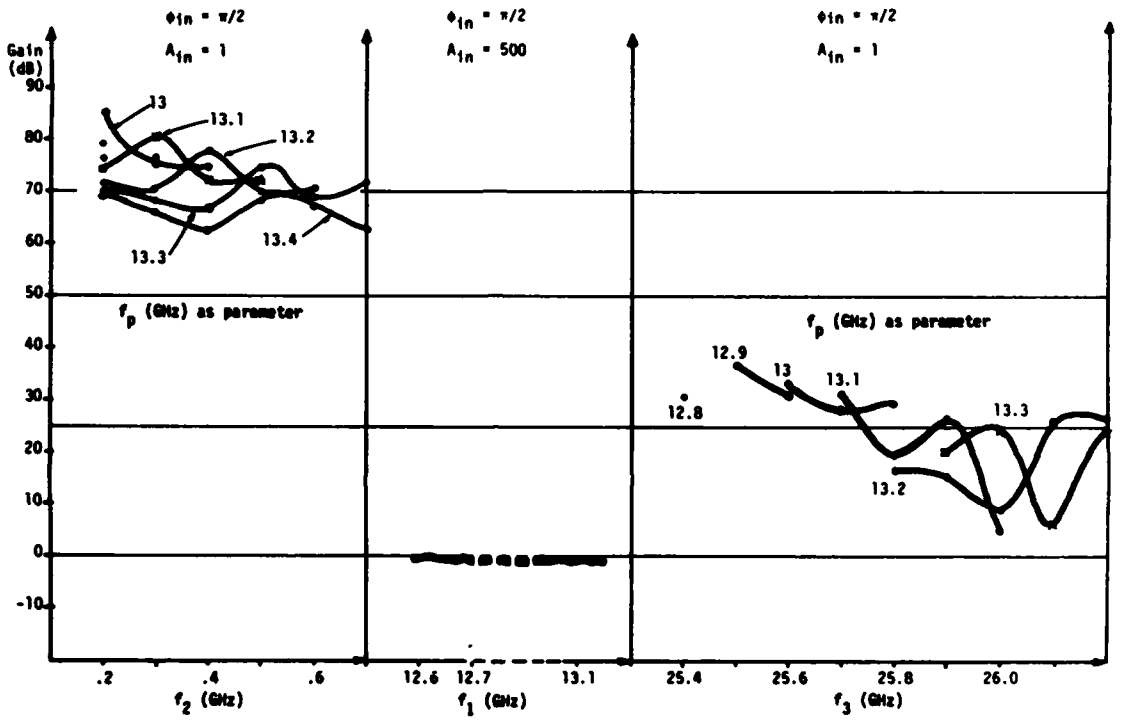

Fig. 8. Power gain versus frequency for all three waves when f_p is close to or in first bandgap.

3.4 Experimental Verification

The computer results obtained predicted that a very-low-frequency component in the spectrum should be present when parametric oscillations are occurring. The measurement of frequency components as low as a few megahertz being impossible at the output of the tube (waveguide output), a coupler was inserted at the input of an S-band tube, and the reflected spectrum measured. Figure 9 shows the low-frequency spectrum reflected from the tube in overdrive condition. A very pure signal is observed at about 50MHz when the tube is operated close to the $\pi/2$ mode. The signal disappears when the overdrive condition is removed, and the frequency of the spectral line is independent of sole or cathode voltage, thus refuting the hypotheses that backward wave oscillations are responsible for this low-frequency content.

Finally, Figure 10 shows the output spectra under the same conditions* (the upper left picture shows the spectrum at the output of the tube, the reflected spectrum being shown in lower left figure). It is seen that the spacing between spectral lines is about 60MHz in both the fundamental and harmonic spectrum, strongly indicating cross modulation between the drive signal and the harmonic signal with the low-frequency component. These lines disappear when normal drive power (30W) is applied.

3.5 Reduced Width of Bandgap (Stopband)

The mathematical model described above shows that the parametric gain decreases when the width of the stopband decreases. It can be shown that excess capacitance or inductance at the end of each bar of the meander line

* The results shown in Figure 10 were obtained from another production tube if compared to Figure 3.

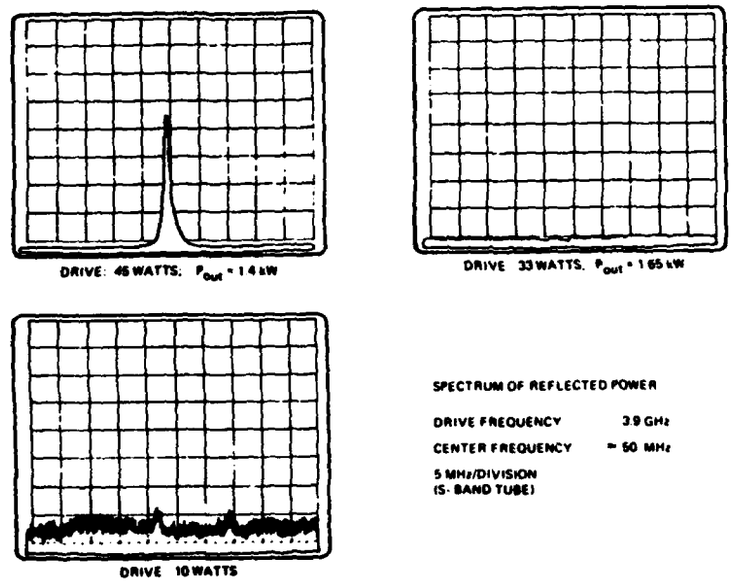

Fig. 9. Spectrum of reflected power.

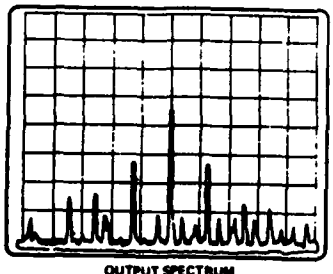

OUTPUT SPECTRUM
CENTER FREQUENCY: 7.8 GHz

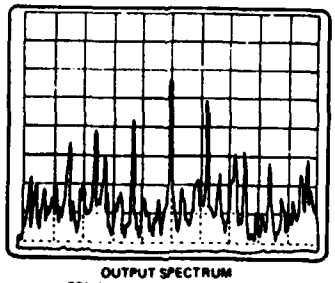

OUTPUT SPECTRUM
CENTER FREQUENCY: 3.9 GHz

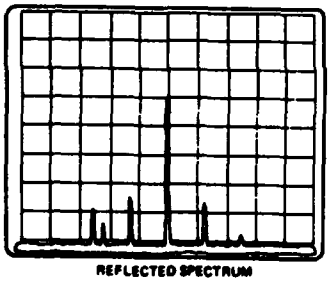

REFLECTED SPECTRUM

OUTPUT POWER AND REFLECTED SPECTRUM
DRIVE FREQUENCY: 3.9 GHz
DRIVE POWER: 45 Watts
50 MHz/DIVISION

Fig. 10. Output power and reflected spectrum.

(finger connections) increases the width of the stopband. Using the simplified model above, the value θ for the phase shift per section can be found from:

$$\cos\theta = \cos\beta\ell_1 + \frac{yZ_o}{2}\sin\beta\ell_2 \qquad (14)$$

θ: phase shift per section
ℓ_1: length of dielectric section
ℓ_2: length of connecting section
y: admittance of unloaded section ℓ_2
Z_o: impedance of loaded section ℓ_1

The stopband occurs whenever the magnitude of cos θ is greater than 1. The first stopband occurs where φ approaches π, and cos θ is less than -1. For larger yZ_o, the stopband is wider, and the parametric gain will be greater.

Some experimental cold-test models were build to determine the effect of possible excess capacitance at the edges of the meander line. The first models were meander lines on flat continuous substrates, with the corners modified as shown in Figure 11. The effect upon the width of the stopband of "clipping the corners" to reduce excess capacitance is shown in Figure 12. The point was never reached at which removing more material would increase the width of the stopband because of excess inductance.

3.6 Conclusion and Discussion (CFA)

The model for parametric oscillations presented here fulfills the basic requirements empirically defined for their existence, namely, the model requires the presence of an electron beam, preferably at full power, and the presence of a drive signal, preferably in overdrive conditions. The model then clearly

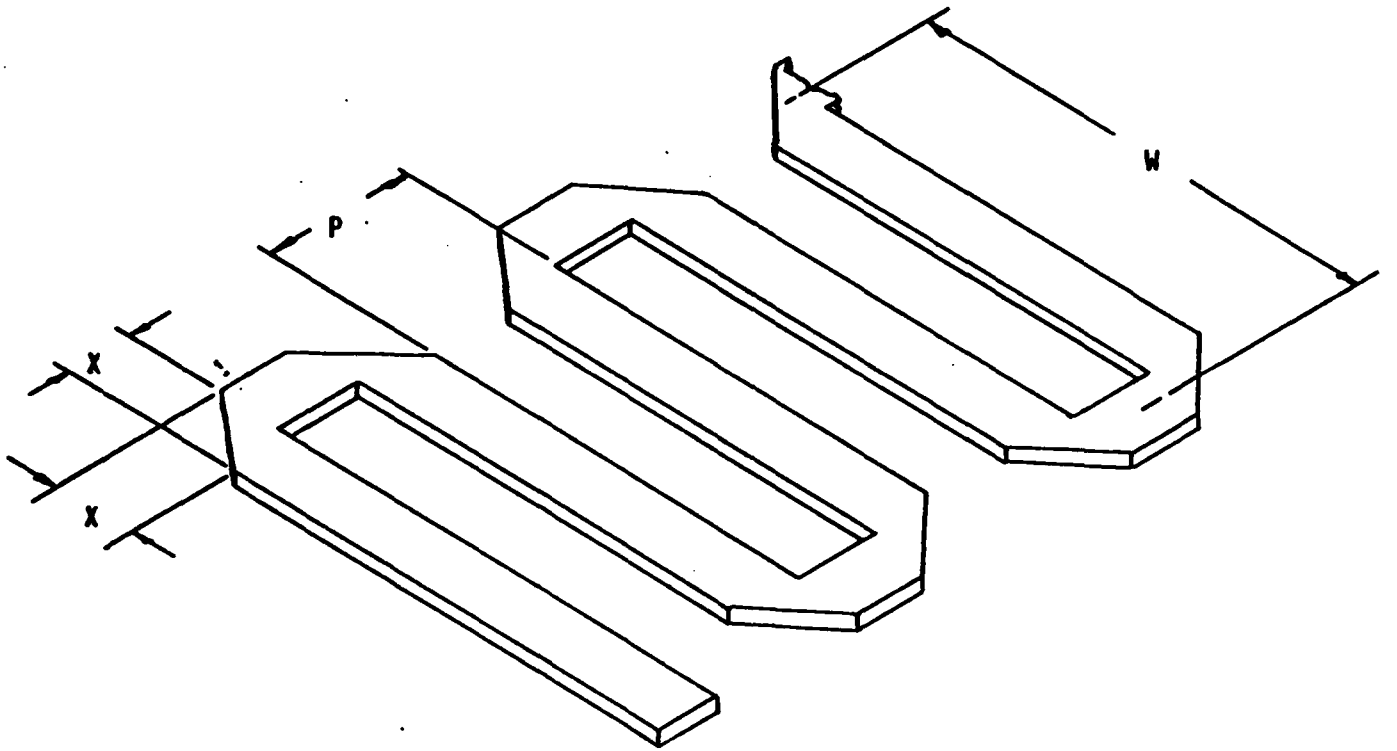

Pitch: p = 0.080"
Width: w = 0.800"
Chamfer at corners: x = 0 to 0.050"

156-022868

Figure 11. Removal of material of meander line to reduce excess capacitance.

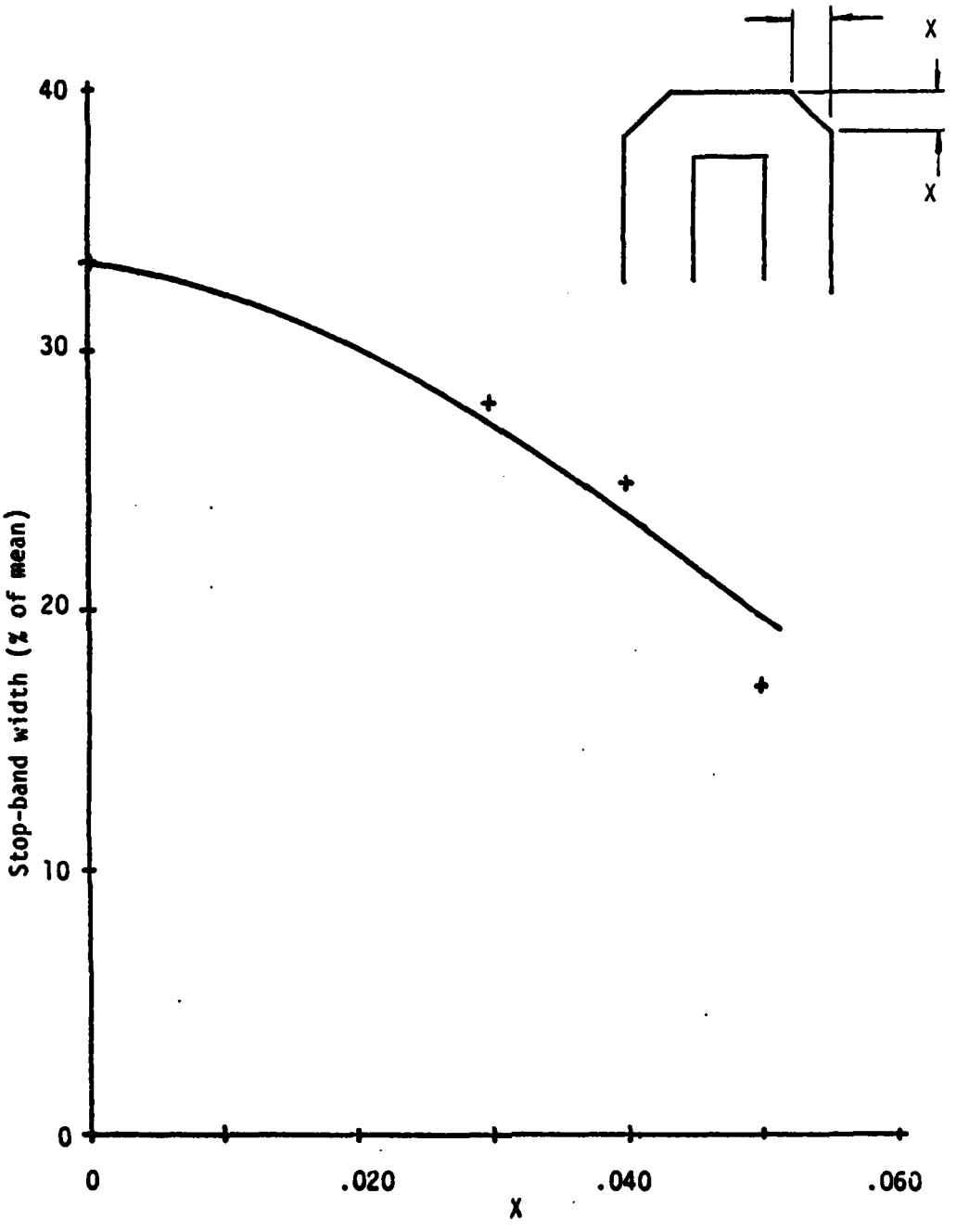

156-022869

Figure 12. Reduction of width of stop-band by reduced capacitance.

defines a fixed frequency f_0 located at the lower edge of the bandgap of the periodic slow wave structure, and predicts the simultaneous existence of a very-low-frequency oscillation. The existence of this low frequency oscillation has been verified experimentally.

The presented model further predicts that power gain is obtained at low frequencies (f_1) and frequencies close to the bandgap (f_2). This power is obtained from the pump signal, and thus apparently from the second harmonic of the drive signal. If it can be shown that power from the fundamental drive signal can be converted to power in the second harmonic, from which power is removed, then the power "suckout" observed frequently would also be explained. Therefore, the necessary further mathematical and experimental evaluation of the present model can only be completed if the direct influence of the electron beam is taken into account.

As described in the interim report, difficulties in computer programming occurred during the first phase of this study. It is only after the introduction of 3 coupled waves that gain could be obtained.

4.0 THE MODEL OF THE O-TYPE TRAVELING WAVE TUBE

4.1 The Physical Model

Figure 13 shows a typical rod supported helix which serves as slow wave structure in many O-type traveling wave tubes. The helix, or spiral, is supported inside a metallic cylinder by a certain number of rods, and an electron beam of cylindrical symmetry moves with a velocity v_e in z-direction inside the helix. The electromagnetic wave, injected at one end of the helix, mainly propagates between the helix and the cylinder (at ground), and therefore propagates in a "quasi" microstrip line with the velocity nearly equal to the velocity of light, c. To advance in z-direction by a distance P equal to the pitch of the helix, the RF wave must travel a distance $\ell = \sqrt{(2\pi R)^2+P^2}$ along the helix. Consequently, the wave advances in z-direction with a reduced velocity $v \simeq cP/\ell$, and synchronism in z-direction between the beam and the wave can be achieved by properly dimensioning the helix.

Considering Figure 13, it is seen that the wave propagates around the helix with a velocity c for a certain distance given by the separation between the rods supporting the helix. As a result, therefore, the RF wave propagates again in a microstrip which is periodically loaded by a dielectric. In Figure 13, the RF wave penetrates and exits a dielectric section three times for each period of the helix.

Similar to the case of the CFA, the electron beam is RF modulated at a frequency f_d and contains all the harmonic frequencies mf_d. Following the discussion in Section 2.0 of this report, the wave at point z will propagate

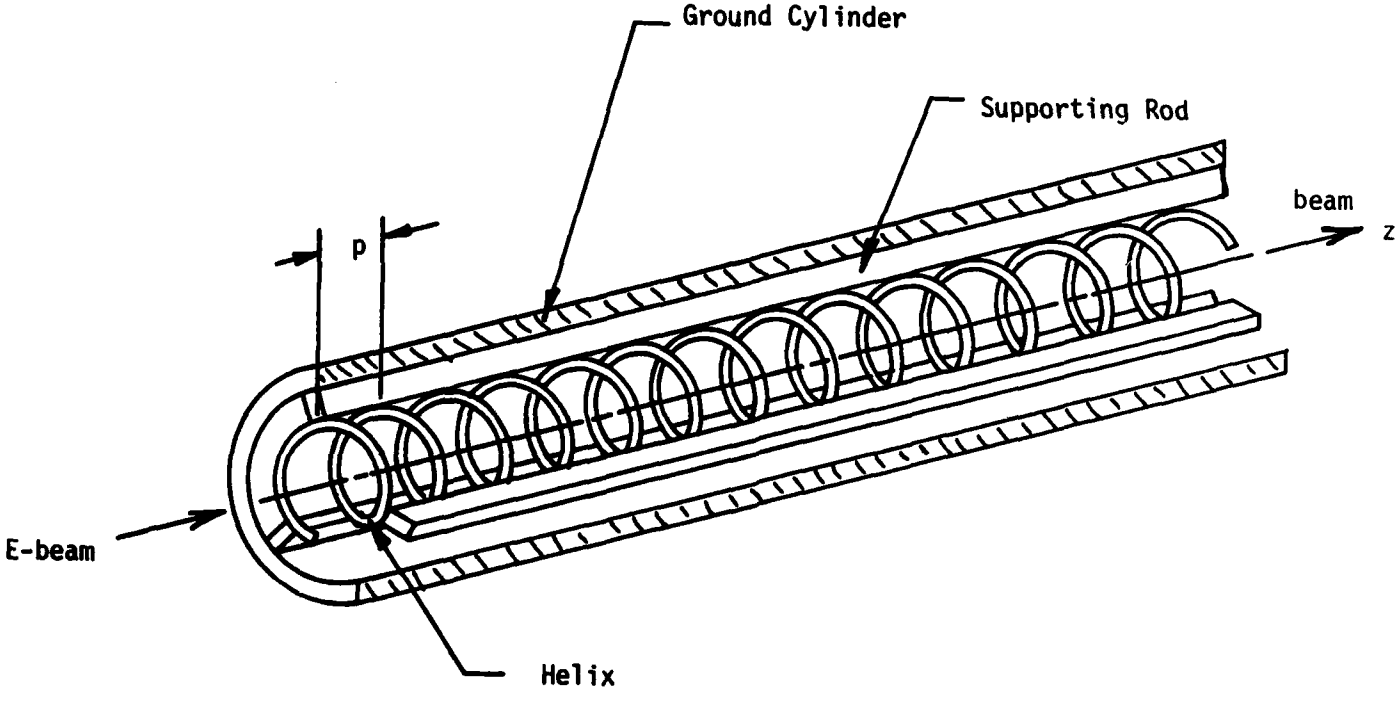

Figure 13. Schematic of TWT interaction space.

in a medium with an effective dielectric constant ε given by*:

$$\varepsilon = \bar{\varepsilon}\,[1 + 2\delta\cos\,\omega_p(t - z/v_e)] \tag{15}$$

$$\omega_p = m\omega_d$$

Since the wave is slowed down by the helix structure, Relation (15) can be simulated by assuming a time and space dependent dielectric constant:

$$\varepsilon = \bar{\varepsilon}\,[1 + 2\delta\cos\,\omega_p(t - z'/\bar{v}_e)] \tag{16}$$

$$\bar{v}_e = v_e\,\ell/P$$

where z' is the travel distance along the helix.

Consequently, if one stretches the helix (as was done previously for the meander line), the RF wave propagates in a microstrip which:

a) is periodically loaded by a (small) dielectric section

b) and whose (effective) dielectric constant varies as given by Equation (16).

This is schematically shown in Figure 14. Comparing Figure 14 with Figure 5, it is seen that the effective dielectric constant of the helix is not only time dependent, as it is in the CFA, but is also dependent on the space coordinate x (which replaces z'). Although similar in principle, both models are different in this respect, and require a different mathematical model.

4.2 The Mathematical Model

4.2.1 Maxwell's Equations

Assuming the wave to propagate in the waveguide shown in Figure 14 to propagate in a TEM mode, the relevant Maxwell's equations become:

$$\partial E/\partial x = -\mu\,\partial H/\partial t; \qquad \partial H/\partial x = +\partial\,\varepsilon E/\partial t$$

* The factor 2 in front of δ was introduced to simplify the following equations.

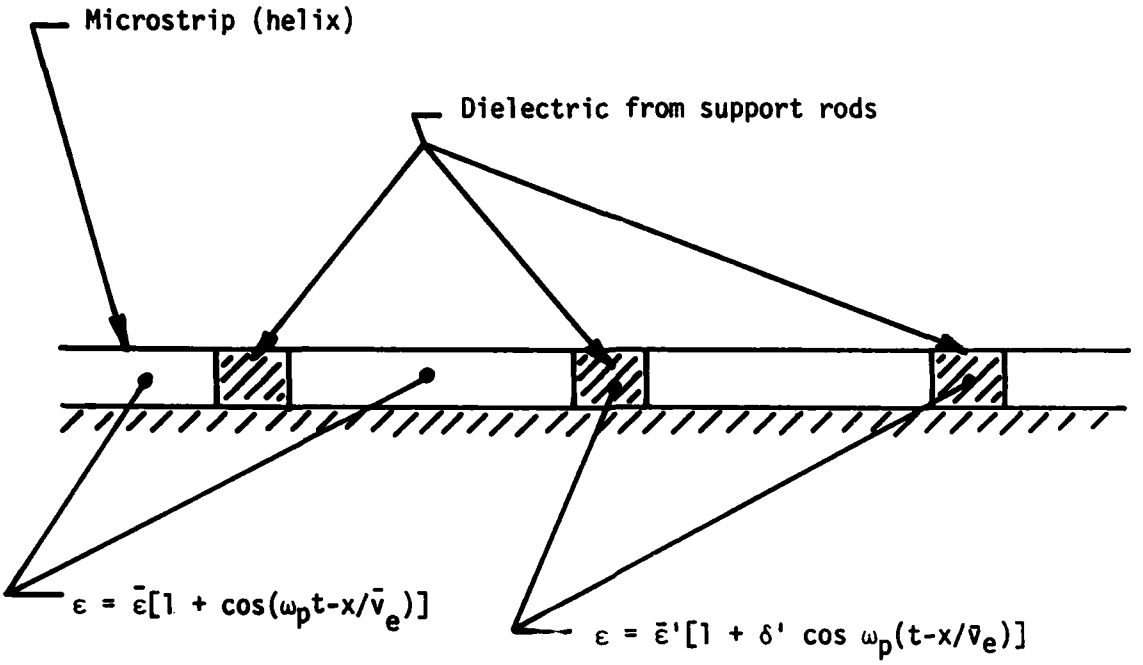

Figure 14. Physical model of the helix structure in O-Type traveling wave tubes (z' was replaced by the coordinate x for simplification).

where ε is the time (t) and space (x) dependent effective dielectric constant for any section of the simulated helix waveguide structure.

For a given frequency ω, the solution for constant ε is obviously given by the "free" modes:

$$\exp j\,(\omega t \pm \beta x) \qquad \beta = \omega\sqrt{\varepsilon\mu} \tag{17}$$

representing waves with the propagation constant β and the phase velocity $\pm c = \pm\,(\varepsilon\mu)^{-1/2}$.

If the dielectric constant depends on time and space:

$$\varepsilon = \bar{\varepsilon}\,[\,1 + 2\delta\cos(\omega_p t - \beta_p x)] \tag{18}$$

$$\beta_p = \omega_p/\bar{v}_e = \omega_p P/\ell v_e = (n\omega_d P)/(\ell v_e)$$

then a single mode (ω,β) will also contain components $\omega + n\omega_p$. Using therefore the Ansatz:

$$E = \Sigma\, E_n \exp j(\omega + n\omega_p)t + \text{c.c.} \tag{19}$$

$$H = \Sigma\, H_n \exp j(\omega + n\omega_p)t + \text{c.c.}$$

where c.c. stands for the complex conjugate values, it follows immediately by insertion:

$$dE_n/dx + j\omega_n \mu H_n = 0 \qquad \omega_n = \omega + n\omega_p \tag{20a}$$

$$dH_n/dx + j\omega_n \bar{\varepsilon} E_n = -j\omega_n \delta\bar{\varepsilon}\left\{E_{n-1}\, e^{-j\beta_p x} + E_{n+1}\, e^{j\beta_p x}\right\} \tag{20b}$$

where the conjugate values have disappeared since each of the equations can be modified by taking its conjugate complex value. As discussed previously for the CFA delay line, if a wave with a single frequency ω is injected into the simulated helix waveguide structure, then waves of all frequencies $\omega_n = \omega + n\omega_p$ will be generated and will propagate within the first section of the periodic waveguide. Contrary, however, to the CFA meander line, these waves will not propagate with a common propagation constant β. Consequently, an accurate mathematical model must keep track of an infinite number of waves in both directions. It is seen, however, from Equation (20b), that the waves generated by the wave ω decrease rapidly in amplitude as n is increased. It is easily shown that the amplitude of the n-th mode related to ω varies proportionally to the n-th power of δ, where δ is small as compared to 1. It is therefore meaningful to consider only the waves with $n = 0$ and $n = \pm 1$.

4.2.2 Active Coupling

Let us consider now the case when two waves of frequencies F_1 and F_2 are injected into the simulated helix waveguide structure. Let us further assume that F_1 and F_2 are chosen in such a way that:

$$F_1 + F_2 = F_p \tag{21}$$

The injection of the wave of frequency ω_1 will lead to the generation of waves with frequency $\omega_1 - \omega_p$ and $\omega_1 + \omega_p$. The value of $\omega_1 - \omega_p$ being equal to $-\omega_2$, and neglecting the term with frequency $\omega_1 + \omega_p$, it follows that the wave of frequency ω_1 is coupled to the wave of frequency ω_2 through the complex value

of the wave at frequency ω_2. Similarly, the wave of frequency ω_2 will generate waves of frequencies $\omega_2 + \omega_p$ and $\omega_2 - \omega_p = -\omega_1$. Thus, the waves of frequency ω_1 and ω_2 are coupled through their complex conjugate values. Using Equations (20), one obtains the 4 equations:

$$dE_1/dx + j\mu\omega_1 H_1 = 0 \tag{22a}$$

$$dH_1/dx + j\bar{\varepsilon}\omega_1 H_1 = -j\delta\bar{\varepsilon}\omega_1 (E_2^* \, e^{-j\beta_p x}) \tag{22b}$$

$$dE_2/dx + j\mu\omega_2 H_2 = 0 \tag{22c}$$

$$dH_2/dx + j\omega_2\bar{\varepsilon}E_2 = -j\delta\omega_2\bar{\varepsilon}(E_1^* \, e^{-j\beta_p x}) \tag{22d}$$

The waves (E_1, H_1) and (E_2, H_2) of frequencies ω_1 and ω_2 are coupled through their complex conjugate values. It can be shown[4] that the waves are actively coupled in this case, meaning that power from (to) the pump can be transferred to (from) the two waves.

4.2.3 Passive Coupling

Let us again assume two waves of frequency F_1 and F_3 to be injected into the simulated waveguide structure. Let us assume now that the two frequencies F_1 and F_3 fulfill the condition:

$$F_3 - F_1 = F_p \tag{23}$$

The injection of the wave of frequency ω_3 will lead to the generation of waves with frequency $\omega_3 - \omega_p = \omega_1$ and $\omega_3 + \omega_p$. Similarly, the wave of frequency ω_1 will generate waves of frequency $\omega_1 + \omega_p = \omega_3$ and $\omega_1 - \omega_p$. If one neglects

the components related to the frequencies $\omega_3 + \omega_p$ and $\omega_1 - \omega_p$, the following relations are obtained from Equations (20):

$$dE_1/dx + j\mu\omega_1 H_1 = 0 \tag{24a}$$

$$dH_1/dx + j\bar{\varepsilon}\omega_1 E_1 = -j\delta\bar{\varepsilon}\omega_1 (E_3 e^{j\beta_p x}) \tag{24b}$$

$$dE_3/dx + j\mu\omega_3 H_3 = 0 \tag{24c}$$

$$dH_3/dx + j\omega_3\bar{\varepsilon}E_3 = -j\delta\bar{\varepsilon}\omega_3 (E_1 e^{-j\beta_p x}) \tag{24d}$$

It is seen in this case that the waves (E_1, H_1) and (E_3, H_3) of frequencies ω_1 and ω_3 are coupled to each other through their corresponding amplitudes. It can be shown[4] that power may be transferred from one wave to the other, but no power is delivered by the pump. Following Louisell[4], these waves are referred to as being passively coupled.

4.2.4 Relationship to Normal Modes

Relations (24a) and (24b) can be combined by multiplying the second relation by the impedance $Z_0 = \sqrt{\mu/\bar{\varepsilon}}$ of the waveguide. If one adds and subtracts the resulting relation from Equation (24a), one obtains the relation:

$$\Delta_{1\pm}\, \phi_{1\pm} = -j\, \frac{\delta}{2} \sqrt{\bar{\varepsilon}\mu}\, \omega_1 \quad (\phi_{3+} + \phi_{3-})\, e^{j\beta p x} \tag{25}$$

where we have introduced the normal modes:

$$\phi_{n\pm} = \frac{E_n \pm Z_0 H_n}{4\sqrt{Z_0}} \tag{26}$$

and the differential operator

$$\Delta_{n\pm} = \frac{d}{dx} \pm j\beta_n \tag{27}$$

Equation (26) is the classical representation of normal modes. The power carried by the mode is $|\phi_{n+}|^2 - |\phi_{n-}|^2$, indicating that ϕ_{n+} is a forward mode, and ϕ_{n-} is a backward mode. This can be easily seen from relation (25) when neglecting coupling. One obtains then:

$$\phi_{1\pm} \sim e^{\pm j\beta_1 x}$$

which corresponds to waves with positive and negative phase velocity.

4.2.5 Parametric Amplification

Let us assume two waves of frequencies ω_1 and ω_2 to propagate in the waveguide, and let us assume that they are actively coupled:

$$\omega_1 + \omega_2 = \omega_p$$

and that their uncoupled propagation constants are β_1 and β_2, such that:

$$\beta_p = \beta_1 + \beta_2 + \bar{\beta}$$

The corresponding normalized coupled mode equations are then given by:

$$\Delta_{1+}\,\phi_{1+} = -j\frac{\delta}{2}\sqrt{\epsilon\mu}\;\omega_1\,\phi_{2+}^{*}\,e^{-j\beta p x} \tag{28}$$

$$\Delta_{2-}\,\phi_{2+}^{*} = j\,\frac{\delta}{2}\sqrt{\epsilon\mu}\;\omega_2\,\phi_1\;e^{j\beta p x}$$

where the conjugate complex of the second equation was taken ($\Delta_+^* = \Delta_-$). In normal mode nomenclature, the coupling coefficient c_{12} from wave 1 to wave 2 and the coupling c_{21} from wave 2 to wave 1 are given by:

$$c_{12} = -j \frac{\delta}{2} \sqrt{\varepsilon\mu}\ \omega_1$$

$$c_{21} = j \frac{\delta}{2} \sqrt{\varepsilon\mu}\ \omega_2$$

showing immediately that the Manley Rowe equations are fulfilled:

$$\frac{c_{12}}{\omega_1} = \frac{c_{21}^*}{\omega_2}$$

Introducing:

$$\beta_1' = \beta_1 + \frac{1}{2}\bar{\beta}$$

$$\beta_2' = \beta_2 + \frac{1}{2}\bar{\beta}$$

and using the Ansatz:

$$\phi_{j+} = A_{j+}\, e^{-j\beta_j' x} \qquad j = 1, 2$$

one obtains by inserting into the system (28):

$$\left(\frac{d}{dx} - j\frac{\bar{\beta}}{2}\right) A_{1+} = c_{12} A_{2+}^*$$

$$\left(\frac{d}{dx} + j\frac{\bar{\beta}}{2}\right) A_{2+}^* = c_{21} A_{1+}$$

Solutions of this system of equations is easily obtained by assuming A_{1+} and A_{2+} to be proportional to exp λx. The Eigen-value λ must satisfy the relation:

$$\lambda = \pm \frac{1}{2} \sqrt{\delta^2 \beta_1 \beta_2 - \bar{\beta}^2} \tag{29}$$

showing that exponential growing waves are obtained for very small values of $\bar{\beta}$. The energy gained by the waves, therefore, must be obtained from the pump. For $\bar{\beta} = 0$, the maximum gain is obtained, namely $\lambda_m = \frac{1}{2} \delta \sqrt{\beta_1 \beta_2}$.

It is interesting to note that exponential gain with a backward wave can be obtained. For $\bar{\beta} \simeq -2\beta_2$ namely, relation (29) can give exponential gain:

$$\lambda = \pm \beta_2 \sqrt{\delta^2 \beta_1 / \beta_2 - 4}$$

However, the maximum gain becomes very small.

4.2.6 Frequency Conversion

Let us now consider the case of two waves of frequency F_1 and F_3 which are passively coupled:

$$F_3 - F_1 = F_p \tag{30}$$

Let us further assume that these waves have uncoupled propagation constant β_1 and β_3 such that:

$$\beta_3 - \beta_1 + \bar{\beta} = \beta_p$$

The corresponding normalized coupled mode equations are easily obtained from equation (24), namely:

$$\Delta_{1+}\phi_{1+} = -j\frac{\delta}{2}\sqrt{\varepsilon\mu}\,\omega_1\,\phi_{3+}\,e^{j\beta_p x}$$

$$\Delta_{3+}\phi_{3+} = -j\frac{\delta}{2}\sqrt{\varepsilon\mu}\,\omega_3\,\phi_{1+}\,e^{-j\beta_p x}$$

As previously shown, the Manley Rowe equations are fulfilled. This system of equations can be solved by using the approach described in Section 4.2.5. We will employ Laplace's transform to demonstrate a more general technique to solve such a system of equations.

If $\bar{\phi}_{j+}(p)$ is the image of $\phi_{j+}(x)$, it follows:

$$(p + j\beta_1)\,\bar{\phi}_{1+}(p) = \omega_1 c\,\bar{\phi}_{3+}(p - j\beta_p)$$

$$(p + j\beta_3)\,\bar{\phi}_{3+}(p) = \omega_3 c\,\phi_{1+}(p + j\beta_p)$$

From the second of these relations, the value $\bar{\phi}_{3+}(p - j\beta_p)$ can be found by replacing p by $p - j\beta_p$. It follows then that $\bar{\phi}_3$ can be eliminated, leading to an equation containing $\bar{\phi}_{1+}$ alone. This relation can only be fulfilled if:

$$p^2 + jp(\beta_1 + \beta_3 - \beta_p) - \beta_1(\beta_3 - \beta_p) - c^2\omega_1\omega_3 = 0$$

leading to:

$$p = -j[\beta_1 + \beta_3 - \beta_p \pm \sqrt{(\beta_1 - \beta_3 + \beta_p)^2 - 4c^2\omega_1\omega_3}] / 2$$

Since c^2 is negative*, it follows that p is always imaginary, so that no instabilities (exponential growth) can occur. In this case, power is transferred back and forth from the two distinct modes ϕ_{1+} and ϕ_{3+}.

* c is purely imaginary

4.2.7 Boundary Conditions

Considering the periodically loaded waveguide shown in Figure 14, it is seen that the waves alternately will propagate in an empty section of the waveguide followed by a "small" section filled with a dielectric. At each of the interfaces between the empty waveguide and the filled waveguide, boundary conditions must be fulfilled. These boundary conditions require the matching of the field components (E, H) for any given frequency. From the definition (26) of the normal modes, it follows that the two functions:

$$E_j = 2\sqrt{Z_0}\,(\phi_{j+} + \phi_{j-}) \tag{31}$$

$$H_j = 2(\phi_{j+} - \phi_{j-})/\sqrt{Z_0}$$

must be continuous at each of the boundaries considered. Note that j indexes the frequency considered.

4.2.8 Conclusion

We have established the mathematical fundamentals of the model proposed for the traveling wave tube in terms of the coupled mode theory. As in the case of the CFA, we will consider waves with three different frequencies, which means that we will have to track 6 waves, 3 in each direction. The boundary conditions (31) must then apply at each of the many interfaces between the empty and filled waveguide sections.

4.3 Three Waves

4.3.1 Basic Relations

We shall consider three waves of frequency F_1, F_2 and F_3 to propagate in each direction. We shall assume that the waves 1 and 2 are actively coupled, and that the waves 1 and 3 are passively coupled, i.e.:

$$F_1 + F_2 = F_p \tag{32}$$

$$F_3 - F_1 = F_p$$

In view of the results obtained in Section 4.2 of this report, it is seen that the "free" propagation constants $\beta_i = \omega_i\sqrt{\varepsilon\mu}$ fulfill equations similar to Equation (32), namely:

$$\beta_1 + \beta_2 = \omega_p\sqrt{\varepsilon\mu} = \bar{\beta}_p \tag{33}$$

$$\beta_3 - \beta_1 = \omega_p\sqrt{\varepsilon\mu} = \bar{\beta}_p$$

where we have introduced $\bar{\beta}_p$ which is not necessarily equal to β_p, the propagation constant of the "dielectric wave", which propagates with a velocity $\bar{v}$ determined mainly by the velocity of the electrons.

Considering the results obtained in Section 4.2, it is seen that a system of 6 differential equations of the first degree must be solved:

$$\Delta_{1\pm}\,\phi_{1\pm} = \mp jc\beta_1(\phi_{2+}^{*} + \phi_{2-}^{*})\exp -j\beta_p x \tag{34a}$$

$$\bar{+}jc\beta_1(\phi_{3+} + \phi_{3-})\exp j\beta_p x$$

$$\Delta_{2\mp}\,\phi_{2\pm}^{*} = \pm jc\beta_2\,(\phi_{1+} + \phi_{1-})\exp j\beta_p x \qquad (34b)$$

$$\Delta_{3\pm}\,\phi_{3\pm} = \mp jc\beta_3\,(\phi_{1+} + \phi_{1-})\exp -j\beta_p x$$

$$\Delta_{i\pm} = (d/dx) \pm j\beta_i; \qquad c = \delta/2$$

The first step in analyzing the proposed model will be to solve this system of equations.

4.3.2 The Dispersion Equation

The system of equations (34) can be Laplace transformed:

$$\bar{\phi}(p) = \int_0^\infty e^{-px}\,\phi(x)\,dx$$

Six equations are then obtained, which contain the image functions $\bar{\phi}_{i\pm}$, some of which with arguments $p \pm j\beta_p$. These image functions can easily be eliminated by shifting p to $p \pm j\beta_p$. Eliminating the functions $\bar{\phi}_{2\pm}$ and $\bar{\phi}_{3\pm}$ leads to two equations for $\bar{\phi}_{1\pm}$:

$$\begin{pmatrix} p + j\beta_1 - \kappa & -\kappa \\ \kappa & p - j\beta_1 + \kappa \end{pmatrix} \begin{pmatrix} \bar{\phi}_{1+}\ (p) \\ \bar{\phi}_{1-}\ (p) \end{pmatrix} = 0$$

which can only be fulfilled if the determinant of the 2 x 2 matrix vanishes. This leads to particular values of $p = -j\beta$, which must fulfill the dispersion equation:

$$\beta^2 - \beta_1^2 = \delta^2\beta_1^2 \left[\frac{\beta_2^2}{(\beta-\beta_p)^2 - \beta_2^2} + \frac{\beta_3^2}{(\beta+\beta_p)^2 - \beta_3^3} \right] \qquad (35)$$

If $\delta = 0$, the "free" solutions $\beta \pm \beta_i$ are obtained. If $\delta \neq 0$, then relation (35) represents a 6th order equation leading to 6 different solutions. This could be predicted since we started with a system of 6 differential equations (34).

In general, δ^2 is very small as compared to 1. Unless at least one term of the denominators of the right hand in (35) nearly vanishes, the solutions of equation (35) are given approximately by $\beta \sim \pm\beta_i$. "Strong" deviations from these solutions can only occur if and only if one or both of the following relations is satisfied:

$$\pm\beta_1 \pm \beta_2 \approx \beta_p$$

$$\pm\beta_1 \pm \beta_3 \approx \beta_p$$

Remembering that β_i are positive values, and considering relation (33), it follows that interaction occurs when either or both the following relations are satisfied:

$$\beta_1 + \beta_2 = \bar{\beta}_p \approx \beta_p$$

$$\beta_3 - \beta_1 = \bar{\beta}_p \approx \beta_p$$

The right hand side of equation (35) will be small as compared to 1 (proportional to δ^2) if β is set approximately equal to $-\beta_1$. Consequently, one can deduce that the backward wave 1 will never be "strongly" coupled to the other waves, and, as such, can be assumed to propagate "free" with the unperturbed propagation constant $-\beta_1$. Similarly, one can deduce that the

backward waves 2 and 3 will also propagate "freely" with their respective propagation constants $-\beta_2$ and $-\beta_3$ respectively. Thus, one can assume the backward waves to propagate as:

$$\phi_{i-} \sim \exp +j\beta_i x$$

If one neglects now the respective coupling terms related to backward waves in the system of equations (34), one finds a dispersion equation of the third order only, namely:

$$\Delta\beta = \frac{\delta^2}{4}\beta_1 \left[\frac{\beta_3}{\Delta\beta + \Delta\beta_p} - \frac{\beta_2}{\Delta\beta - \Delta\beta_p}\right] \tag{36}$$

$$\Delta\beta = \beta - \beta_1; \qquad \Delta\beta_p = \beta_p - \bar{\beta}_p$$

This relation merits some discussion. Consider the following cases:

(a) Neglect wave 3 ($\beta_3 = 0$)

The solution corresponds then to the solution obtained earlier for actively coupled waves 1 and 2:

$$\Delta\beta = (\Delta\beta_p/2) \pm j\sqrt{\delta^2\beta_1\beta_2 - \Delta\beta_p^2}\ /\ 2$$

Under synchronism ($\Delta\beta_p = 0$), maximum gain for the exponential waves are obtained.

(b) Neglect wave 2 ($\beta_2 = 0$)

The solution corresponds to the solution obtained earlier for passively coupled waves 1 and 3:

$$\Delta\beta = -(\Delta\beta_p/2) \pm j\sqrt{\Delta\beta_p^2 + \delta^2\beta_1\beta_3}\ /\ 2$$

In this case, no growing waves are obtained.

(c) Synchronism ($\beta_p = \bar{\beta}_p$)

In this case, it is easily seen that the solutions become:

$$\beta_1 \text{ and } \beta_1 \pm s; \quad s = (\delta/2)\sqrt{\beta_1(\beta_3 - \beta_2)} \tag{37}$$

Since it can be shown that $\beta_3 - \beta_2 = 2\beta_1$, no growing waves can be expected. In view of the growing waves one obtains between actively coupled waves, this result seems surprising. However, the passively coupled mode dominates the actively coupled mode, and power is essentially converted among the various waves.

(d) General case (assynchronism)

In the general case of assnychronism ($\Delta\beta_p \neq 0$), it can be shown that growing waves will exist if the synchronism factor $\Delta\beta_p$ is slightly positive or negative. Under certain conditions, discussed in Appendix 1, the imaginary part of β becomes:

$$\text{Im}(\beta) = \pm .24\ \delta\bar{\beta}_q \tag{I.6}$$

$$(\beta_q/\beta_1 >> 1)$$

In general, however, one must solve the dispersion equation (36) to obtain the exact values of the solutions β_i.

4.3.3 The General Solution

Representing the solutions of the dispersion equation (36) to be

$$\Delta\beta = s_1, s_2, s_3$$

then the most general solution for the three waves is obtained by using the ansatz:

$$\phi_{1+} = \left(\sum_{1}^{3} A_n \, e^{-jsnx} \right) e^{-j\beta_1 x} \tag{38a}$$

Inserting this value into relations (34b) and (34c) and keeping in mind that coupling from and to backward waves is neglected, leads to:

$$\phi_{2+}^{*} = c\beta_2 \left(\sum_{1}^{3} \frac{A_n \, e^{-jsnx}}{\Delta\beta_p - s_n} \right) \exp j(\beta_2 + \Delta\beta_p)x \tag{38b}$$

$$\phi_{3+} = c\beta_3 \left(\sum_{1}^{3} \frac{A_n \, e^{-jsnx}}{\Delta\beta_p + s_n} \right) \exp -j(\beta_3 + \Delta\beta_p)x \tag{38c}$$

where the coefficients A_n are determined by boundary conditions. For example, the knowledge of $\phi_{i+}(0)$ for all three waves ($i = 1, 2, 3$) at $x = 0$ uniquely determines A_n.

4.3.4 Conclusion

The most general solution has been determined when 3 waves of frequencies F_1, F_2 and F_3 are propagating in each direction in a given section of a waveguide. Two of these waves were assumed to be actively coupled, and two of these waves were assumed to be passively coupled. The simultaneous presence

of all three waves does not lead to exponential growing waves when perfect synchronism is assumed. A certain value of the asynchronism factor $\overline{\Delta\beta}_p$, however, leads to exponential growing waves. The sensitivity of the synchronism factor $\Delta\beta_p$ on the exponential growth of the waves may explain the extreme sensitivity of the "power suck-out" to external and internal tube parameters, such as beam voltage and assymmetry in the placement of the helix supporting rods.

A generalized theory with these three waves requires solving a dispersion equation of the six-th order. Simplification results when no coupling from and to the backward waves is assumed. The third order dispersion equation leads to three solutions, two of which can be complex conjugate. The general solution (38) must then be applied to each section of the waveguide, and proper boundary condition introduced. This requires again a complex computer code, and the results will not be explicative from the physics point of view. Since two actively coupled waves lead to exponential growing waves, we will apply in the next section the boundary conditions to waves F_1 and F_2 which are actively coupled (Section 5.0).

5.0 PARAMETRIC TWT AMPLIFICATION

5.1 General

In order to understand the physics involved in both the cases of CFA and the TWT, we will consider in this section two actively coupled waves such that:

$$\omega_1 + \omega_2 = \omega_p \tag{39}$$

$$\beta_1 + \beta_2 = \beta_p$$

It follows then from the discussion in Section 4.0 that the general solution of the system containing 4 waves (2 in each direction) is given by:

$$\phi_{1+} = (a_1 e^{sx} + a_2 e^{-sx}) \exp -j\beta_1 x \tag{40a}$$

$$\phi_{1-} = b_1 \exp j\beta_1 x \tag{40b}$$

$$\phi_{2+}^{*} = jc\frac{\beta_2}{s}(a_1 e^{sx} - a_2 e^{-sx}) \exp +j\beta_2 x \tag{40c}$$

$$\phi_{2-}^{*} = b_2 \exp -j\beta_2 x \tag{40d}$$

$$s = c\sqrt{\beta_1\beta_2} = \frac{\delta}{2}\sqrt{\beta_1\beta_2}$$

where a_1 and b_1 are constants of integration.

Let us define the vector:

$$\vec{\psi} = (\phi_{1+}, \phi_{1-}, \phi_{2+}^{*}, \phi_{2-}^{*}) \tag{41}$$

It is then easy to define the transformation matrices for a single section of the waveguide.

5.2 The Transformation Matrices

5.2.1 Transformation Through a Single Empty Waveguide Section of Length ℓ_1

Figure 14 shows the schematic of the waveguide to be analyzed. Let us assume that the "entrance" of a single empty waveguide section is located at $x = 0$, so that the "exit" of the empty waveguide section is located at $x = \ell_1$, see Figure 15.

If the value of the vector $\vec{\psi}$ at $x = 0$ is known (see definition 41), then the value of $\psi(\ell_1)$ in the empty waveguide can be easily determined by using the relations (40). One obtains a transformation matrix (L_1) which transforms the vector ψ such that:

$$\vec{\psi}(\ell_1) = (L_1)\psi(0) \tag{42}$$

where L_1 is defined in Figure 16. This matrix can be decomposed into a matrix (L_{1_0}) representing the transmission in the absence of pumping ($s = 0$) and a coupling matrix (S_1) which describes the coupling through the pump frequency ω_p.

5.2.2 Interface Boundary Condition

The boundary conditions (31) must now be applied at the interface between the vacuum and the dielectric (see Figure 15). The vectors $\vec{\psi}$ at the position $x = \ell_1 - \Delta$ and at the position $x = \ell_1 - \Delta$ $(\Delta \to \varepsilon)$ can be related to each other by a transformation matric (B_0):

$$\vec{\psi}(\ell_1 - \Delta) = (B_0)\,\vec{\psi}\,(\ell_1 + \Delta) \tag{43}$$

where (B_0) is defined in Figure 17. We are now in the position to relate directly $\vec{\psi}(\ell_1)$ in the dielectric to the initial vector $\psi(0)$ in the vacuum by the transformation:

$$\vec{\psi}(\ell_1) = (B_0^{-1})\,(L_1)\,\vec{\psi}\,(0)$$

Note that B_0 is a transformation matrix which does not depend on the pump wave ω_p.

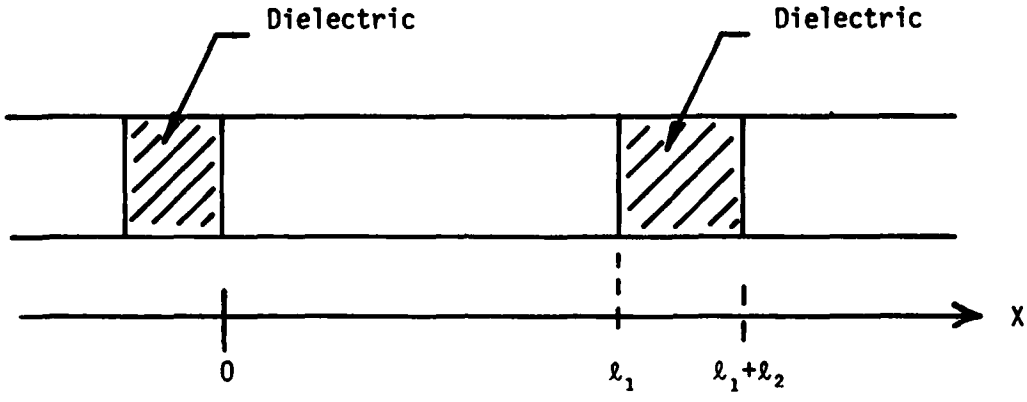

Figure 15: Single waveguide section.

$$L_1 = \begin{bmatrix} e^{-j\beta_1 \ell_1}\cosh s\ell_1 & 0 & -\kappa e^{-j\beta_1 \ell_1}\sinh s\ell_1 & 0 \\ 0 & e^{j\beta_1 \ell_1} & 0 & 0 \\ -e^{j\beta_2 \ell_1}(\sinh s\ell_1)/\kappa & 0 & e^{j\beta_2 \ell_1}\cosh s\ell_1 & 0 \\ 0 & 0 & 0 & e^{j\beta_2 \ell_1} \end{bmatrix}$$

$$\kappa = js/c\beta_2$$

$$L_{10} = \begin{bmatrix} e^{-j\beta_1 \ell_1} & 0 & 0 & 0 \\ 0 & e^{j\beta_1 \ell_1} & 0 & 0 \\ 0 & 0 & e^{j\beta_2 \ell_1} & 0 \\ 0 & 0 & 0 & e^{-j\beta_2 \ell_1} \end{bmatrix}$$

$$S_1 = \begin{bmatrix} \cosh s\ell_1 & 0 & -\kappa \sinh s\ell_1 & 0 \\ 0 & 1 & 0 & 0 \\ -\sinh s\ell_1/\kappa & 0 & \cosh s\ell_1 & 0 \\ 0 & 0 & 0 & 1 \end{bmatrix}$$

Figure 16. The transformation matrix (L_1) which can be represented by the product (L_1) = (L_{10})(s_1).

$$(B_0) = \begin{pmatrix} B_1 & 0 \\ 0 & B_1 \end{pmatrix}$$

$$(B_1) = \frac{1}{2\epsilon^{1/4}} \begin{pmatrix} 1 + \sqrt{\epsilon} & 1 - \sqrt{\epsilon} \\ 1 - \sqrt{\epsilon} & 1 + \sqrt{\epsilon} \end{pmatrix}$$

Figure 17. The 4 x 4 boundary transformation matrix (B_0) decomposed into 2 x 2 matrices.

5.2.3 Transformation Through the Dielectric Section

The behavior of the solution in the dielectric portion is similar to the behavior of the solutions in the vacuum section if one replaces β_i by k_i, where $k_i = \beta_i/\sqrt{\varepsilon_d}$, ε_d being the dielectric constant of the dielectric material. To be exact, the solution of the dispersion equations will be $\pm\bar{s}_1$, where $\bar{s}_1$ is either real or imaginary, depending on the synchronization factor. Therefore, the transformation matrix through the dielectric section (L_2) will be similar to the transformation matrix (L_1). We will assume that ℓ_2 is so small, that the coupling matrix (S_2) is nearly equal to unity:

$$\vec{\psi}(\ell_1 + \ell_2) = (L_2)\,\vec{\psi}\,(\ell_1) \tag{44}$$

$$(L_2) = (L_{20})\,(S_2) \approx (L_{20})$$

where the transformation matrix (L_{20}) is shown in Figure 18 (and should be compared to Figure 16).

5.2.4 The Transformation Through a Complete Single Section

If one applies a boundary condition transformation similar to the one given by relation (43), one finds that the transformation one has to apply is just given by B_0. Consequently, it follows that $\vec{\psi}(\ell_1 + \ell_2) = \vec{\psi}(p)$ at the entrance of a vacuum section can be related to the vector $\vec{\psi}(0)$ of the following section through a transformation matrix given by:

$$\vec{\psi}(p) = (B_0)\,(L_{20})\,(S_2)\,(B_0^{-1})\,(L_{10})\,(S_1)\,\vec{\psi}\,(0) \tag{45}$$

$$(L_{20}) = \begin{bmatrix} e^{-jk_1\ell_2} & 0 & 0 & 0 \\ 0 & e^{jk_1\ell_2} & 0 & 0 \\ 0 & 0 & e^{jk_2\ell_2} & 0 \\ 0 & 0 & 0 & e^{-jk_2\ell_2} \end{bmatrix}$$

$$(S_2) = \begin{bmatrix} \cosh\bar{s}_1\ell_2 & 0 & -\bar{\kappa}\sinh\bar{s}_1\ell_2 & 0 \\ 0 & 1 & 0 & 0 \\ -\sinh\bar{s}_1\ell_2/\bar{\kappa} & 0 & \cosh\bar{s}_1\ell_2 & 0 \\ 0 & 0 & 0 & 1 \end{bmatrix} \approx I$$

Figure 18. The 4 x 4 transmission matrix $(L_2) \approx (L_{20})\ (s_2) \approx (L_{20})$ through the dielectric.

which, as discussed earlier, can be simplified by setting $(S_2) \approx (I)$:

$$\vec{\psi}(p) = (T_0)\,(S_1)\,\vec{\psi}(0) \tag{46}$$

$$(T_0) = (B_0)\,(L_{20})\,(B_0^{-1})\,(L_{10})$$

where (T_0) is the unperturbed transformation matrix one obtains when coupling (pumping) between the waves is neglected.

5.2.5 The Complete Transformation Matrix

It is clear that if N individual sections are present, then one can relate the input vector $\vec{\psi}(0)$ to the helix to the output vector $\vec{\psi}(Np)$ of the helix by successive transformations (46) to obtain:

$$\vec{\psi}(Np) = (T_0 S_1)^N\,\vec{\psi}(0) \tag{47}$$

We note here that (T_0) is the inperturbed transformation matrix, and that (T_0) is multiplied by a coupling matrix (S_1) which is nearly equal to the unit matrix $s\ell_1 << 1$. It is therefore of interest to discuss the matrix To before solving relation (47).

5.3 The Unperturbed Matrices

In the absence of the coupling, i.e., $(S_1)=I$, both waves of frequencies ω_1 and ω_2 will propagate uncoupled through the periodic waveguide structure. Consequently, the 4 x 4 matrix (T_0) can be reduced to 2 x 2 matrices $Z(i)$ such that:

$$T_0 = \begin{pmatrix} Z(1) & 0 \\ 0 & Z(2) \end{pmatrix} \tag{48}$$

where Z(i) represents the transformation of a single wave of frequency ω_i. The matrix Z can be calculated rather easily, and one finds the matrix shown in Figure 19. This matrix fulfills the condition Det Z = |Z| = 1, and, following Cowley Hamilton's relation, can be represented by:

$$Z = I \cos\theta + K \sin\theta \tag{49}$$

where θ is defined by:

$$\cos\theta = \frac{1}{2}(Z_{11} + Z_{22}) = \text{Real } Z_{11}$$

$$= \cos\beta\ell_1 \cos k\ell_2 - \frac{1+\varepsilon}{2\sqrt{\varepsilon}} \sin\beta\ell_1 \sin k\ell_2 \tag{50}$$

and K given by:

$$K \sin\theta = \begin{pmatrix} \frac{Z_{11} - Z_{22}}{2} & Z_{12} \\ Z_{21} & -\frac{Z_{11} - Z_{22}}{2} \end{pmatrix} \tag{51}$$

It can be shown rather easily that:

$$K^2 = -I; \quad Z^n = I \cos n\theta + K \sin n\theta \tag{52}$$

where I is the unit matrix.

Relation (51) describes the ω-β diagram. If the right hand side of Equation (50) is larger than or equal to 1, then θ becomes imaginary, and no propagation can occur in a waveguide made up of many individual periodic sections.

If θ is real, then relation (51) describes Floquet's theorem: the waves suffer a net phase shift θ per single section.

Of interest for later use are the eigenvalues λ and the eigenvectors $\vec{\xi}$ of the matrix Z. It is easily seen that the relation:

$$Z\vec{\xi}_n = \bar{\lambda}_n \vec{\xi}_n$$

can be verified for:

$$\bar{\lambda}_1 = \bar{\lambda}_2^* = e^{j\theta} \tag{53}$$

$$\vec{\xi}_{1,2} = (-K_{12}, \; K_{11} \mp j)$$

showing that each wave $\vec{\xi}_{1,2}$ is phase shifted through the N sections of the helix:

$$\vec{\xi}_{1,2}\,(\text{out}) = e^{\pm jn\theta}\, \vec{\xi}_{1,2}\,(\text{in})$$

Note that the eigenvalues fulfill the second order equation:

$$\bar{\lambda}^2 - 2\bar{\lambda}\cos\theta + 1 = 0 \tag{54}$$

It follows therefore that the unperturbed matrix T_0 in equation (48) has the 4 eigenvalues $\bar{\lambda}_1$, $\bar{\lambda}_2 = \bar{\lambda}_1^*$, $\bar{\lambda}_3$, $\bar{\lambda}_4 = \bar{\lambda}_3^*$, where $\bar{\lambda}_{1,2}$ are the eigenvalues associated with the matrix Z(1), i.e., the frequency ω_1, and $\bar{\lambda}_{3,4}$ are the eigenvalues associated with the matrix Z(2), i.e., the frequency ω_2. The eigenvectors of the matrix T_0 are then given by:

$$\vec{\xi}_{1,2} = [-K_{12}(1), \; K_{11}(1) \mp j, \; 0, \; 0] \tag{55}$$

$$\vec{\xi}_{3,4} = [0, \; 0, \; -K_{12}(2), \; K_{11}(1) \mp j]$$

$$\lambda_{1,2} = e^{\pm j\theta_1}; \qquad \lambda_{3,4} = e^{\pm j\theta_2}$$

5.4 General Method of Solution

The general method which will be applied to solve relation (47) will be as follows:

1) determine the 4 eigenvalues Δ_i of the matrix $T = T_0 S_1$

2) determine the 4 eigenvectors $\vec{\sigma_i}$ of the matrix $T = T_0 S_1$

3) decompose the input vecotr $\vec{\psi}(0)$ into 4 eigenvectors $\sum_1^4 \alpha_n \vec{\sigma}_n$

4) apply the multiplication rule:

$$T^N \psi(0) = \sum_1^4 \alpha_n \Delta_n^N \vec{\sigma}_n$$

5) compare the resulting vector to the vector $\vec{\psi}(Np)$

When applying the multiplication rule, let us assume that $\Delta_r = \lambda_n(1 + \varepsilon_n)$, then:

$$T^N \psi(0) = \sum_1^4 \alpha_n \lambda_n^N (1 + \varepsilon_n)^N \vec{\sigma}_n$$

so that gain can be expected whenever $|1 + \varepsilon_n| > 1$, since:

$$(1 + \varepsilon)^N = \exp [N \ln (1 + \varepsilon_n)] \approx \exp N\varepsilon_n$$

One can therefore expect a power gain G whenever the real part of ε_n is positive. The gain G will then be given by:

$$G_n = 8.7 \text{ N Real } \varepsilon_n \qquad (56)$$

5.5 Results and Discussion

It can be shown that the 4 eigenvalues Δ_n of the transformation matrix must fulfil a 4th order equation which is discussed in Appendix II. This 4th order equation with complex coefficients has been numerically solved by computer. With $N \simeq 100$, small gain of a few hundreds to a few tenths of a dB were generally obtained* except in the vicinity of $\theta_{1,2} \simeq k\pi$. In this case, a double or quadruple solution was expected, and inaccuracies in the computer code were evident. However, gains in excess of 100 dB were calculated.

A general discussion on the eigenvalues is made in Appendix II. Of primary importance are the two parameters θ_1 and θ_2, which describe the actual phase shift of the waves F_1 and F_2 through a single waveguide section. Different cases are considered.

Case I - General Case: $k\pi \neq \theta_1 \neq \theta_2 \neq n\pi$

The gain obtained in this general case is relatively small, being proportional to the square of the amplitude of the dielectric modulation (i.e. $\sim \delta^2$). Since δ is small compared to 1, no appreciable gain is obtained. This was verified by computer code.

Case II - The π modes (θ_1 or $\theta_2 \simeq k\pi$, but $\theta_1 \neq \theta_2$)

It is shown in Appendix II that if one of the waves is a π mode, then a gain proportional to δ is obtained. This leads to a gain of a few dB's, as verified by the computer.

Case III - Dual and Equal π modes ($k\pi = \theta_1 = \theta_2 + 2n\pi$)

Maximum gain is obtained when both waves are π (or $n\pi$) modes. The gain here is found to be proportional to the square root of δ and, with the values $\delta = 10^{-2}$, $\varepsilon \simeq 5$, $\ell_2/\ell_1 \simeq 10\%$, gains in excess of 100 dB's were calculated.

* Computer evaluation was made by using $\delta \simeq 10^{-2}$, $\varepsilon \simeq 5$, $\ell_2/\ell_1 \simeq 10\%$

As shown in Appendix II, the relevant values of ε_n [$\Delta_n = \lambda_n(1 + \varepsilon_n)$] are approximately given by:

$$\varepsilon_n^2 = \pm \frac{\varepsilon - 1}{2\sqrt{\varepsilon}} \sinh(\delta\sqrt{\beta_1\beta_2}\, \ell_1/\ell_2)A \qquad (57)$$

$$A^2 = (\sin\beta_1\ell_1 \sin\beta_2\ell_1)$$

Relation (57) has been confirmed within 20% error by computer calculations. It is surprising to find the gain to be proportional to $\delta^{1/2}$

Case IV - Dual and Opposite π modes: ($k\pi = \theta_1 = \theta_2 + (2n + 1)\pi$)

The gain one obtains in this case is porportional to δ, and corresponds to the single π mode case. This case is important, however, since it can directly be related to the results obtained for the CFA.

In the case of the CFA, maximum gain was obtained when F_1 was first at the lower edge of the first band gap ($\theta_1 \simeq \pi$). A very low frequency oscillation ($F_2 \simeq 50$ MHz) was then determined. This corresponds to $\theta_2 \simeq 0$.

It can therefore be expected that even higher gains can be obtained in the case of the CFA is both θ_1 and θ_2 are set equal to $k\pi$ modes ($\theta_1 = k\pi$, $\theta_2 = \theta_1 + 2n\pi$). This case was not analyzed as yet: the approximations made for the CFA evaluation do not allow to set $F_1 = F_2$.

6.0 CONCLUSIONS AND FUTURE WORK

The general model, proposed by Northrop and supported by AFOSR, for the occurence of parametric oscillations in high power microwave amplifiers has been applied to both injected beam crossed field amplifiers and traveling wave tubes. The results obtained clearly indicate that the model can describe the effects of one class of spurious oscillations observed experimentally.

In the case of the CFA, a constant frequency located within the first band gap has been identified. The occurence of the spurious oscillation has been linked to a very low frequency oscillation. This low frequency oscillations has been observed experimentally, and was shown not to be correlated to backward wave oscillation. Experimentally the band gap of meander lines has been reduced by properly matching the finger end connections. The results have been published in 2 publications[2,3].

The model of the TWT was simplified in order to obtain a better understanding of these oscillations. The occurrence of simultaneous π modes leads to gains of the order of 100 dB's or more. The analysis carried out in this report implicitely assumes perfect synchronism ($\beta_1 + \beta_2 = \beta_p$). In general, this is not the case. Appendix III shows the dispersion equation for the assynchronism. A detailed analysis should be made using the proper dispersion equation.

A basis for the occurence of parametric oscillations has been established. If it can be shown that power from the fundamental drive signal can be converted to power in the second or higher order harmonic from which power is removed to build up the parametric waves, then the "power suck-out" observed frequently would be explained. This subject should be investigated, together with a correlation between experimental data and the theoretical predictions made in this report.

APPENDIX 1

The Dispersion Equation

The dispersion equation (38) can be written in normalized form:

$$x^3 + 3px + 2q = 0 \qquad \text{(I.1)}$$

$$p = -\frac{1}{3}[y^2 + 1]; \quad q = yz$$

$$x = \Delta\beta(\sqrt{2}/\delta\beta_1); \quad y = \sqrt{2}\Delta\beta_p/\delta\beta_1; \quad z = \bar{\beta}_q/2\beta_1$$

The relevant parameter to discuss is:

$$\kappa = p^3 + q^2 = -\frac{1}{27}(y^2 + 1)^3 + y^2z^2 \qquad \text{(I.2)}$$

If κ is positive, then one real and 2 conjugate complex solutions exist. Let us therefore discuss the possibility of conjugate complex solutions.

In order to obtain growing waves, one must fulfill the condition:

$$\left(\frac{y^2 + 1}{3}\right)^3 < y^2z^2 \qquad \text{(I.3)}$$

In order to discuss this condition, let us discuss the value for κ. For $y = 0$, κ is equal to -1/27, and is negative. The maxima (and minima) of κ as a function of y are determined by the condition:

$$\frac{\partial\kappa}{\partial y} = 0$$

which leads to the following conditions:

$$\text{(a)}\quad y = 0 \qquad\qquad \kappa < 0$$

$$\text{(b)}\quad y^2 + 1 = \pm 3z$$

Condition (a) is without direct interest, since $\kappa < 0$. Condition (b) requires y^2 to be positive, and therefore:

$$y^2 = 3z - 1 > 0$$

Inserting this value for y into (I.2) leads to the condition:

$$\kappa_m = z^2\,(2z - 1)$$

which is always fulfilled since $2z = \bar{\beta}_q/\beta_1$ and the waves are actively coupled. It follows therefore that exponential growing waves will always exist if the "synchronism" factor y is set equal to

$$y = \pm \sqrt{3z - 1}$$

and it is clear that a certain "bandwidth" $\Delta\beta_p$ exists around this value in which growing waves exist. If κ is positive, then one usually defines the two parameters u and v given by:

$$u^3 = -q + \sqrt{\kappa}; \qquad v^3 = -q - \sqrt{\kappa} \tag{I.4}$$

and the 3 solutions are then given by:

$$x_1 = u + v; \quad x_{2,3} = -\frac{u + v}{2} \pm j\frac{\sqrt{3}}{2}(u - v) \tag{I.5}$$

Maximum gain is therefore obtained when κ is maximally positive, i.e., for $\kappa = \kappa_m$. An estimate for the maximum gain can be obtained when $\kappa = \kappa_m$.

$$u^3 = z[\sqrt{3z - 1} + \sqrt{2z - 1}]$$

$$v^3 = z[\sqrt{3z - 1} - \sqrt{2z - 1}]$$

which shows that z must be chosen as large as possible. Since $z = \bar{\beta}_q/\beta_1$, it is seen that β_1 must be chosen as small as possible. For large values of z, one obtains:

$$u^3 \approx z\sqrt{z}\,(\sqrt{3} + \sqrt{2}) \approx (1.47z)^3$$

$$v^3 \approx z\sqrt{z}\,(\sqrt{3} - \sqrt{2}) \approx (.68z)^3$$

and the maximum gain will become:

$$\frac{\sqrt{3}}{2}(u - v) \approx \frac{\sqrt{3}}{2} z\,(1.47 - .68) = .68z$$

$$= .34\,\bar{\beta}_q/\beta_1$$

In terms of $\Delta\beta$, it follows then that:

$$\text{Jm}\,\beta_{max} = \Delta(.34\,\bar{\beta}_q/\beta_1)\frac{\delta\beta_1}{\sqrt{2}} = .24\delta\bar{\beta}_q \qquad \text{(I.6)}$$

APPENDIX II

Eigenvalues of $(T_0 S_1)$

It can be shown rather easily that the 4 eigenvalues Δ_i of the transformation matrix $(T_0 S_1)$ have to fulfil the following 4th order equation:

$$[\Delta^2 - \Delta(Z_{11}(1)\cosh x + Z_{22}(1)) + \cosh x] \cdot \qquad \text{(A2.1)}$$

$$\cdot [\Delta^2 - \Delta(Z_{11}^*(2)\cosh x + Z_{22}^*(2)) + \cosh x] +$$

$$- \sinh x^2 [1 - \Delta Z_{11}(1)] [1 - \Delta Z_{11}^*(2)] = 0$$

with $x = s\ell_1$

If one assumes now that $\cosh s\ell_1 \ll 1$, one finds easily:

$$(\Delta - \lambda_1)(\Delta - \lambda_2)(\Delta - \lambda_3)(\Delta - \lambda_4) - \sinh x^2[1 - \Delta Z_{11}(1)][1 - \Delta Z_{11}^*(2)] = 0 \qquad \text{(A2.2)}$$

where the λ_i are the eigenvaleus of the unperturbed transmission Matrix T_0, namely:

$$\lambda_1 = \exp j\theta_1; \qquad \lambda_2 = \exp -j\theta_1 \qquad \text{(A2.3)}$$

$$\lambda_3 = \exp j\theta_2; \qquad \lambda_4 = \exp -j\theta_2$$

Physically, λ_1 and λ_2 are given by the phase shift θ_1 a wave of frequency ω_1 will suffer through one single but complete section of the periodic waveguide. Similarly, θ_2 is the phase shift a wave of frequency ω_2 suffers through one single but complete section of the periodic waveguide.

We expect the eigenvalues Δ_j of the dispersion equation (A2.1) to be close to the eigenvalues λ_j of the unperturbed matrix. Therefore, we will use the ansatz:

$$\Delta_j = \lambda_j(1 + \varepsilon_j) \tag{A2.4}$$

The terms $1 - \Delta_j Z_{11}$ in relation (A2.2) can then be simplified:

$$1 - \Delta_j Z_{11} \approx 1 - \lambda_j Z_{11}$$

and one finds:

$$\begin{aligned}
1 - \lambda_1 Z_{11}(1) &= -\frac{\lambda_1}{2}(\lambda_1 - \lambda_2)(1 - jK_{11}(1)) \\
1 - \lambda_2 Z_{11}(1) &= \frac{\lambda_2}{2}(\lambda_1 - \lambda_2)(1 + jK_{11}(1)) \\
1 - \lambda_3 Z_{11}^*(2) &= -\frac{\lambda_3}{2}(\lambda_3 - \lambda_4)(1 + jK_{11}(2)) \\
1 - \lambda_4 Z_{11}^*(2) &= \frac{\lambda_4}{2}(\lambda_3 - \lambda_4)(1 - jK_{11}(2))
\end{aligned} \tag{A2.5}$$

These relations show the importance of the value of K_{11}, i.e., Z_{11}. The real part of Z_{ii} was given in relation (50), namely:

$$\text{Real } Z_{11} = \text{Real } Z_{22} = \cos\theta \tag{A2.6}$$

$$\cos\theta = \cos\beta\ell_1 \cos k\ell_2 - \sigma \sin\beta\ell_1 \sin k\ell_2$$

$$\sigma = (1 + \varepsilon)/2\sqrt{\varepsilon}$$

ε = dielectric constant

Similarly, the imaginary part of Z_{11} can be evaluated:

$$\mathrm{Im}Z_{11} = -\mathrm{Im}Z_{22} = -jK_{11}\sin\theta \qquad \text{(A2.7)}$$

$$= -(\cos\beta\ell_1 \sin k\ell_2 + \sigma \sin\beta\ell_1 \cos k\ell_2)$$

Furthermore, since the determinant of the matrix (Z) is equal to 1:

$$Z_{11}Z_{22} - Z_{12}Z_{21} = 1$$

One finds easily with $Z_{11} = Z_{22}^{*} = \cos\theta + K_{11}\sin\theta$

$$-(K_{11}^2 + 1)\sin^2\theta = Z_{12}Z_{21} = \frac{(\varepsilon - 1)^2}{4\varepsilon}\sin^2\beta\ell_1$$

resulting in the relation:

$$K = \pm j\sqrt{\frac{1 + (\varepsilon - 1)^2 \sin^2\beta\ell_1}{4\varepsilon \sin^2\theta}} \qquad \text{(A2.8)}$$

ε = dielectric constant

Clearly, relations (A2.8) and (A2.7) show that K_{11} may become infinite as θ approaches $k\pi$, and that the product

$$\frac{\lambda_3 - \lambda_4}{2}(1 + jK_{11}) = j\sin\theta\,(1 + jK_{11})$$

approaches the value $-\sin\theta\, K_{11}$ as $\theta \to k\pi$. For $\theta = k\pi$, the value stays generally finite if $\beta\ell_1 \neq k\pi$.

We will now differentiate between cases.

Case I: $\lambda_i \neq \lambda_j$ $(i \neq j)$

In this case, the eigenvalues of the unperturbed matrix are all different from each other. Using (A2.4) and (A2.5) one finds:

$$\varepsilon_1 = -\sinh^2 x\,[1 - jK_{11}(1)]\,\frac{1 - \lambda_1 Z_{11}^*(2)}{2(\lambda_1 - \lambda_3)(\lambda_1 - \lambda_4)}$$

$$\varepsilon_2 = -\sinh^2 x\,[1 + jK_{11}(1)]\,\frac{1 - \lambda_2 Z_{11}^*(2)}{2(\lambda_2 - \lambda_3)(\lambda_2 - \lambda_4)} \qquad \text{(A2.9)}$$

$$\varepsilon_3 = -\sinh^2 x\,[1 + jK_{11}(2)]\,\frac{1 - \lambda_3 Z_{11}(1)}{2(\lambda_3 - \lambda_1)(\lambda_3 - \lambda_2)}$$

$$\varepsilon_4 = -\sinh^2 x\,[1 - jK_{11}(2)]\,\frac{1 - \lambda_4 Z_{11}(1)}{2(\lambda_4 - \lambda_1)(\lambda_4 - \lambda_2)}$$

It is seen that ε_j is proportional to the square of the depth of modulation δ ($\sinh x \approx x = \delta\sqrt{\beta_1\beta_2}\,\ell_1/2$), and as such, relatively low gain will be obtained. It is interesting to note that K_{11} can become infinite for $\sin\theta \sim 0$. In this case, however, λ_1 and λ_2 are nearly equal, so that the case of the π modes must be considered.

Case II: The singular π mode

Let us assume that θ_1 is nearly equal to $k\pi$, and that $\theta_2 \neq k\pi$. To solve the dispersion equation, let us set:

$$\lambda_2 = \lambda_1(1 + \S_2) \approx \cos\theta_1 = \pm 1$$

$$|\S_2| \ll 1, \qquad \lambda_1 \neq \lambda_3$$

Let us solve again the dispersion equation (A2.2) with the ansatz:

$$\Delta = \lambda_1(1 + \varepsilon_1)$$

The first term in equation (A2.2) becomes equal to:

$$\lambda_1^2\, \varepsilon(\varepsilon - \S_2)(\lambda_1 - \lambda_3)(\lambda_1 - \lambda_4)$$

The second term of the same equation can be evaluated by using the following relations: $(\S \to 0)$

$$1 - \lambda_1(1 + \varepsilon_1)\, Z_{11}(1) = (1 + \varepsilon_1)\,[1 - \lambda_1 Z_{11}(11)] - \varepsilon_1$$

$$= (1 + \varepsilon_1)\left[-\frac{\lambda_1}{2}\,(\lambda_1 - \lambda_2)\,(1 - jK_{11}(1))\right] - \varepsilon_1$$

$$\simeq -\lambda_1 K_{11}(1)\sin\theta_1 - \varepsilon_1 \simeq -j\lambda_1 \mathrm{Im}Z_{11}(1)$$

Consequently, with $\lambda_1 \approx \pm 1$, one obtains:

$$\varepsilon(\varepsilon - \S_2) = -j\,\frac{\sinh^2 x}{2}\,\mathrm{Im}Z_{11}(1)\,\frac{1 - Z_{11}^{*}(2)}{1 \mp \cos\theta_2} \qquad \text{(A2.10)}$$

$$= -j\,\frac{\sinh^2 x}{2}\left(\mathrm{Im}Z_{11}(1)\right)\left[\pm 1 + \frac{j\mathrm{Im}Z_{11}(2)}{1 \mp \cos\theta_2}\right]$$

For $\S \to 0$, it follows that ε is proportional to sinhx. It is interesting to note, however, that the right hand of equation (A2.7) can become infinitely large if the denominator $1 \mp \cos\theta_2$ vanishes. This occurs for $\cos\theta_2 = 2\pi k$ if $\theta_1 = 2\pi k'$,

or for $\cos\theta_2 = (2k + 1)\pi$ if $\theta_1 = (2k' + 1)\pi$. Therefore, it is expected that a maximum value of ϵ will be obtained when $\theta_1 \approx \theta_2 + 2k\pi$ and $\theta_1 \approx n\pi$. We will consider in the following the dual π modes.

Case III: The dual π modes

The dual π modes will be characterized by:

$$\theta_1 = \theta_2 + 2k\pi = n\pi$$

To solve the equation (A2.2), we will use the ansatz:

$$\Delta = \lambda_1(1 + \epsilon_1)$$

$$\lambda_i = \lambda_1(1 + \S_i) \quad i \geq 2$$

Similar to the discussion above, one finds for the left term in equation (A2.2):

$$\lambda_1^4\, \epsilon_1(\epsilon_1 - \S_2)(\epsilon_1 - \S_3)(\epsilon_1 - \S_4)$$

and the right term of the same equation can be evaluated by using the two relations.

$$1 - \lambda Z_{11}(1) \approx -j\lambda_1(\mathrm{Im}Z_{11}(1))$$

$$1 - \lambda(Z_{11}^*(2)) \approx j\lambda_1 \mathrm{Im}Z_{11}(2)$$

It follows therefore that the equation (A2.2) becomes:

$$\epsilon_1(\epsilon_1 - \S_2)(\epsilon_1 - \S_3)(\epsilon_1 - \S_4) = \sinh^2 x\ \mathrm{Im}Z_{11}(1)\ \mathrm{Im}(Z_{11}(2)) \qquad \text{(A2.11)}$$

which results for perfect synchronism ($\theta_1 = \theta_2 = k\pi$):

$$\epsilon_1^2 = \pm \sinh x \sqrt{[\mathrm{Im}\, Z_{11}(1)\ \mathrm{Im}Z_{11}(2)]} \qquad \text{(A2.12)}$$

From the condition that the determinant of the matrix (Z) is equal to 1, namely:

$$(\text{Real}(Z_{11}))^2 + (\text{Im}(Z_{11}))^2 - Z_{12}Z_{21} = 1$$

and that Real $(Z_{11}) = \pm 1$ at $\theta \simeq k\pi$, it follows that:

$$\text{Im}(Z_{11}) = \pm \sqrt{Z_{12}Z_{21}} = \pm \frac{\varepsilon - 1}{2\sqrt{\varepsilon}} \sin\beta\ell_1$$

and:

$$\varepsilon_1^2 = \pm \frac{\varepsilon - 1}{2\sqrt{\varepsilon}} \sinh x \left[\pm \sin\beta_1\ell_1 \sin\beta_2\ell_1\right]^{1/2} \qquad \text{(A2.13)}$$

Relation (A2.13) shows that ε_1 is proportional to the square root of $\sinh x \sim x$, showing that large gains can be obtained.

APPENDIX III

Non-Synchroneous Case

Equation (39) in Section 5.0 required the synchronism of the two waves, i.e., the wavevector β_p of the pump wave was set equal to the sum of the two wavevectors β_1 and β_2. Physically, this means that the waves are in complete synchronism within the empty waveguide sections. However, under these conditions, the pump wave will advance during the passage of the waves F_1 and F_2 through the dielectric section. Therefore, the second relation of (39) is not necessarily fulfilled. Instead, one must write:

$$\beta_p = \beta_1 + \beta_2 + \Delta\beta \tag{A3.1}$$

Following the approval shown in Section 5.0, one finds then that the value of s must be replaced by:

$$s' = \frac{1}{2}\sqrt{\delta^2\beta_1\beta_2 - \Delta\beta^2} \tag{A3.2}$$

as derived in Section 4.0. Furthermore, it is easily shown that the coupling matrix (s_1) in relation (46) must be replaced by a matrix (s_1') given by:

$$s_1' = \begin{bmatrix} \alpha_1 & 0 & \alpha_2 & 0 \\ 0 & 1 & 0 & 0 \\ \alpha_3 & 0 & \alpha_1^* & 0 \\ 0 & 0 & 0 & 1 \end{bmatrix} \tag{A3.3}$$

with

$$\alpha_1 = [\cosh s'\ell_1 + j \frac{\Delta\beta}{2s'} \sinh s'\ell_1] \exp - j \frac{\Delta\beta}{2} \ell_1$$

$$\alpha_2 = j \frac{\delta\beta_1}{2s'} \sinh s'\ell_1 \exp - j \frac{\Delta\beta}{2} \ell_1 \qquad \text{(A4.4)}$$

$$\alpha_3 = -j \frac{\delta\beta_2}{2s'} \sinh s'\ell_1 \exp j \frac{\Delta\beta}{2} \ell_1$$

Consequently, the 4th order equation for the Eigenvalues (see Equation A2.1) will become:

$$[\Delta^2 - \Delta(Z_{11}(1)\,\alpha_1 + Z_{22}(1)) + \alpha_1] \cdot \qquad \text{(A3.5)}$$

$$[\Delta^2 - \Delta(Z_{11}^*(2)\,\alpha_1^* + Z_{22}^*(1)) + \alpha_1^*] +$$

$$- \alpha_2\alpha_3 [1 - \Delta Z_{11}(1)] [1 - \Delta Z_{11}^*(2)] = 0$$

Note that:

$$\alpha_2\alpha_3 = \frac{\delta^2\beta_1\beta_2}{4s'^2} \sinh^2 s'\ell_1 \qquad \text{(A3.6)}$$

$$\alpha_1\alpha_1^* - \alpha_2\alpha_3 = 1$$

Let us assume now that $\alpha_1 \simeq \alpha_1^* \simeq 1$. One obtains then the equation:

$$(\Delta - \lambda_1)(\Delta - \lambda_2)(\Delta - \lambda_3)(\Delta - \lambda_4) = \frac{\delta^2\beta_1\beta_2}{4s'} \sinh s'\ell_1 \cdot$$

$$\cdot [1 - \Delta Z_{11}(1)][\Delta - \Delta Z_{11}^*(2)]$$

UNCLASSIFIED

SECURITY CLASSIFICATION OF THIS PAGE (When Date Entered)

REPORT DOCUMENTATION PAGE

READ INSTRUCTIONS BEFORE COMPLETING FORM

1. REPORT NUMBER: AFOSR-TR-80-0228	2. GOVT ACCESSION NO.
3. RECIPIENT'S CATALOG NUMBER: rept.	
4. TITLE (and Subtitle): Parametric Oscillations In High Power Microwave Amplifiers	5. TYPE OF REPORT & PERIOD COVERED: Final Jul 77 - Jun 79
	6. PERFORMING ORG. REPORT NUMBER
7. AUTHOR(s): Gunter Dohler	8. CONTRACT OR GRANT NUMBER(s): F49620-77-C-0096
9. PERFORMING ORGANIZATION NAME AND ADDRESS: Northrop Corporation, Defense Systems Division, Electron Tube Section, 175 W. Oakton St, Des Plaines, IL 60018	10. PROGRAM ELEMENT, PROJECT, TASK AREA & WORK UNIT NUMBERS: 2305/C1, 61102F
11. CONTROLLING OFFICE NAME AND ADDRESS: AFOSR/NE, Bolling AFB, D.C. 20332	12. REPORT DATE: 1979
	13. NUMBER OF PAGES: 77
14. MONITORING AGENCY NAME & ADDRESS (if different from Controlling Office): 80	15. SECURITY CLASS. (of this report): UNCLASSIFIED
	15a. DECLASSIFICATION/DOWNGRADING SCHEDULE

16. DISTRIBUTION STATEMENT (of this Report)

Approved for public release; distribution unlimited.

17. DISTRIBUTION STATEMENT (of the abstract entered in Block 20, if different from Report)

18. SUPPLEMENTARY NOTES

19. KEY WORDS (Continue on reverse side if necessary and identify by block number)

crossed field amplifier (CFA)

20. ABSTRACT (Continue on reverse side if necessary and identify by block number)

A CFA model for parametric oscillations was developed which fulfills the basic requirements, empirically defined, for their existence; namely, the model requries the presence, preferably in overdrive conditions. The model then defines a fixed frequency f sub o located at the lower edge of the bandgap of the periodic slow wave structure, and predicts the simultaneous existence of a very-low-frequency oscillation. The existence of this low frequency oscillation has been verified experimentally. The presented model further predicts that power gain is obtained at low frequencies (f sub 1) and frequencies close to the bandgap (f sub 2).

DD FORM 1 JAN 73 1473

409984

UNCLASSIFIED

This power is obtained from the pump signal, and thus apparently from the second harmonic of the drive signal. The mathematical fundamentals of the model proposed for the traveling wave tube in terms of the coupled-mode theory was established. As in the case of the CFA, waves with three different frequencies were considered which means that 6 waves will have to be tracked, 3 in each direction. The boundary conditions must then apply at each of the many interfaces between the empty and filled waveguide sections.